



January 2016

# On The Development Of Novel Multifunctional Max Reinforced Polymers (MRPS) Matrix Composites

Sujan Kumar Ghosh

Follow this and additional works at: <https://commons.und.edu/theses>

---

## Recommended Citation

Ghosh, Sujan Kumar, "On The Development Of Novel Multifunctional Max Reinforced Polymers (MRPS) Matrix Composites" (2016). *Theses and Dissertations*. 2019.  
<https://commons.und.edu/theses/2019>

This Thesis is brought to you for free and open access by the Theses, Dissertations, and Senior Projects at UND Scholarly Commons. It has been accepted for inclusion in Theses and Dissertations by an authorized administrator of UND Scholarly Commons. For more information, please contact [zeinebyousif@library.und.edu](mailto:zeinebyousif@library.und.edu).

**ON THE DEVELOPMENT OF NOVEL MULTIFUNCTIONAL MAX  
REINFORCED POLYMERS (MRPs) MATRIX COMPOSITES**

by

Sujan Kumar Ghosh

Bachelor of Science, Khulna University of Engineering & Technology, Khulna, 2012

A Thesis

Submitted to the Graduate Faculty

of the

University of North Dakota

In partial fulfillment of the requirements

for the degree of

Master of Science

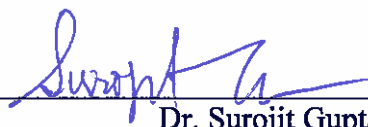
Grand Forks, North Dakota

December

2016

Copyright 2016 Sujan Kumar Ghosh

This thesis, submitted by Sujan Kumar Ghosh in partial fulfillment of the requirements for the Degree of Master of Science from the University of North Dakota, has been read by the Faculty Advisory Committee under whom the work has been done and is hereby approved.



Dr. Surojit Gupta, Ph. D.

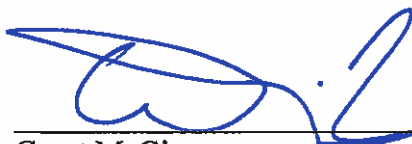


Dr. Matthew Cavalli, PhD., P.E.



Dr. Clement Tang, Ph.D.

This thesis meets the standards for appearance, conforms to the style and format requirements of the Graduate School of the University of North Dakota, and is hereby approved.



Grant McGimpsey  
Dean of the Graduate School

December 12, 2016

Date 12/01/2016

## **PERMISSION**

Title            On the Development of Novel Multifunctional MAX Reinforced Polymers (MRPs)  
Matrix Composites

Department    Mechanical Engineering

Degree         Master of Science

In presenting this thesis in fulfillment of the requirements for a graduate degree from the University of North Dakota, I agree that the library of this University shall make it freely available for inspection. I further agree that permission for extensive copying for scholarly purposes may be granted by the professor who supervised my thesis work or, in his absence, by the chairperson of the department or the dean of the School of Graduate Studies. It is understood that any copying or publication or other use of this thesis or part thereof for financial gain shall not be allowed without my written permission. It is also understood that due recognition shall be given to me and to the University of North Dakota in any scholarly use which may be made of any material in my thesis.

Signature    Sujan Kumar Ghosh

Date            12/01/2016

## TABLE OF CONTENTS

LIST OF FIGURES.....	vii
LIST OF TABLES.....	ix
ACKNOWLEDGEMENTS.....	x
ABSTRACT .....	xi
CHAPTER	
I. INTRODUCTION.....	1
1.1 MAX Phases.....	1
1.2 Background Study of Polymer Matrix Composites.....	3
1.3 Introduction MAX Reinforced Polymers (MRPs).....	4
II. Synthesis and Tribological Behavior of Novel Wear Resistant PEEK-Ti <sub>3</sub> SiC <sub>2</sub> Composites.....	10
2.1 Introduction.....	10
2.2 Experimental Methods.....	11
2.3 Result and Discussion.....	15
2.3.1 Investigation of Microstructures.....	15
2.3.2 Tribological Behavior.....	15

2.3.3 Investigation of Tribosurfaces and Potential Mechanism.....	18
2.4 Conclusion .....	19
III. Novel Self Lubricating Teflon-Ti <sub>3</sub> SiC <sub>2</sub> and Nylon-Ti <sub>3</sub> SiC <sub>2</sub> Composites.....	21
3.1 Introduction.....	21
3.2 Experimental Methods.....	25
3.3 Result and Discussion.....	26
3.3.1 Investigation of Microstructures.....	26
3.3.2 Tribological Behavior.....	31
3.3.3 Investigation of Tribosurfaces and Potential Mechanism.....	34
3.6 Conclusions.....	39
IV. SCOPE FOR FUTURE STUDIES.....	40
4.1 Conclusion.....	40
4.2 Scope of Future Studies.....	41
4.3 Experimental Methods.....	41
4.4 Result and Discussion.....	43
APPENDIX.....	45
REFERENCES.....	45
Chapter I.....	45
Chapter II.....	46
Chapter III.....	48
Chapter IV.....	51
Status of Journal Publications.....	53
Contributed Presentations During Master's Degree.....	53

## LIST OF FIGURES

Figure	Page
1.1. Possible combination of MAX phases.....	1
1.2. Unit Cell for 211(a), 312 (b) and 413 (c) series of MAX phases.....	2
1.3. Predicted and experimental result of tensile modulus of jute-reinforced PP composites.....	3
1.4. Tribological performance of MAX phases at room temperature.....	5
1.5. Mechanical Performances of Epoxy-Ti <sub>3</sub> SiC <sub>2</sub> composites.....	6
1.6. Tribological performances of Epoxy-Ti <sub>3</sub> SiC <sub>2</sub> composite against Inconel 718 substrate.....	7
2.1. SEM SE image of the polished surface of (a) PEEK-5%Si PEEK (inset shows the SEM SE polished surface of PEEK) surface, (b) BSE image of the same region, (c) PEEK-10%Si PEEK, (d) BSE image of the same region, (e) PEEK-20%Si PEEK, (f) BSE image of the same region, (g) PEEK-30%Si PEEK, and (h) BSE image of the same region.....	16
2.2. Plot of (a) porosity (Y1 axis) and Hardness (Y2 axis), (b) friction coefficient ( $\mu$ ) versus distance, (c) mean friction coefficient ( $\mu_{\text{mean}}$ ), and (d) total WR versus PEEK concentration (vol%) of different PEEK-Ti <sub>3</sub> SiC <sub>2</sub> composites.....	17
2.3. SEM SE images of (a) PEEK (inset shows the schematics of adhesive wear), (b) PEEK-20%Si (inset show the schematics of lubricous and WR Type IIIa tribofilm), (c) BSE image of the same region, and (d) higher magnification of the encircled region in (c) after tribology testing (the chemistry of micro-constituent region 1 is $*(\text{Ti}_{0.8}\text{Si}_{0.2})\text{O}_{0.03}\{\text{Cx}\}*$ .....	19
3.1. SE SEM micrographs (a) Teflon, (b) Teflon-5%Si, (c) BSE image of the same region, (d) Teflon-10%Si, (e) BSE image of the same region, (f) Teflon-20%Si, (g) BSE image of the same region, (h) Teflon-30%Si, and (i) BSE image of the same region.....	27

3.2. SE SEM micrographs (a) Nylon, (b) Nylon-5% $\text{Ti}_3\text{SiC}_2$ , (c) BSE image of the same region, (d) Nylon-10% $\text{Ti}_3\text{SiC}_2$ , (e) BSE image of the same region, (f) higher magnification of the marked region, (g) Nylon-20% $\text{Ti}_3\text{SiC}_2$ , (h) BSE image of the same region, and (i) BSE image of Nylon-30% $\text{Ti}_3\text{SiC}_2$ .....	28
3.3. Plot of Porosity (Y1 axis) and Hardness (Y2 axis) versus $\text{Ti}_3\text{SiC}_2$ additions for (a) Teflon- $\text{Ti}_3\text{SiC}_2$ , and (b) Nylon- $\text{Ti}_3\text{SiC}_2$ composites.....	29
3.4. Plot of friction coefficient versus ( $\mu$ ) sliding distance of different compositions of (a) $\text{Ti}_3\text{SiC}_2$ -Teflon, (b) $\text{Ti}_3\text{SiC}_2$ -Nylon, and (c) mean friction coefficient ( $\mu\text{m}$ ) versus $\text{Ti}_3\text{SiC}_2$ additions (vol%) (data of $\text{Ti}_3\text{SiC}_2$ -UHMWPE [22] and $\text{Ti}_3\text{SiC}_2$ -PEEK [23] composites are also inserted in the plot to show comparison).....	30
3.5. Plot of (a) WR versus $\text{Ti}_3\text{SiC}_2$ additions (data of UHMWPE- $\text{Ti}_3\text{SiC}_2$ and PEEK- $\text{Ti}_3\text{SiC}_2$ is inserted for comparison [22-23]), and WR versus friction coefficient of different, (b)Teflon-based composites [Table 1], and (c) Nylon-based composites against Different substrates.....	32
3.6. SE SEM micrographs of (a) Teflon (block), (b) Teflon (disk), (c) Teflon-20% $\text{Ti}_3\text{SiC}_2$ (block), (d) BSE image of the same region (inset shows the higher magnification of the region marked in (d)), (e) Teflon-20% $\text{Ti}_3\text{SiC}_2$ (disk), and (f) BSE image of the same region after tribological testing.....	35
3.7. SE SEM micrographs of (a) Nylon (block), (b) Nylon (disk), (c) Nylon-20% $\text{Ti}_3\text{SiC}_2$ (block), (d) BSE image of the same region, (e) Teflon-20% $\text{Ti}_3\text{SiC}_2$ (disk), and (f) BSE image of the same region after tribological testing (inset shows the higher magnification of the region marked in (f)).....	36
3.8. Schematics of (a1) adhesive wear in polymer-polymer composites, (a2) SEM micrograph showing adhesive wear (Fig. 3.6), (b1) Type IIIa tribofilms, (b2) SEM micrograph showing Type IIIa tribofilm [22], (c1) Negligible mass transfer between tribocouples, (c2) SEM micrograph of Teflon-20% $\text{Ti}_3\text{SiC}_2$ surface (Fig. 3.6), (d1) Abrasive wear at tribocontacts due to the pull out of $\text{Ti}_3\text{SiC}_2$ particulates, and (d2) SEM micrograph showing abrasive wear (Fig. 3.7).....	38
4.1. Plot of Porosity versus MAX phase content.....	43
4.2. Plot of Hardness versus MAX phase content.....	44

## LIST OF TABLES

Table	Page
1.1: A novel method of classifying tribofilms [2] .....	9
2.1: Summary of tribological behavior of PEEK samples.....	12
2.2: The surface roughness before and after the tribological testing.....	14
3.1: Summary of WR and friction coefficient of different PTFE-based tribocouples.....	22
3.2: Summary of WR and friction coefficient of different Nylon-based tribocouples.....	23

## **ACKNOWLEDGEMENTS**

I am grateful to my colleagues, Ross Dunnigan and Faisal AlAnazi, for without them this work would not have been possible. I would like to express my sincerest gratitude to Dr. Surojit Gupta at the University of North Dakota for all of the aid, support and guidance I received during my studies.

In addition, I would like to thank Faisal Riyad for his previous work and my family and friends for their supports during my master's study.

## ABSTRACT

During this thesis, the design and development of novel multifunctional MAX reinforced polymer (MRPs) matrix composites was studied. MRPs were fabricated with a certain volumetric ratio of polymers and MAX phases. In Chapter II, synthesis and tribological behavior of PEEK-Ti<sub>3</sub>SiC<sub>2</sub> composites have been reported. A decrease in friction coefficient is observed when 10 volumetric % of Ti<sub>3</sub>SiC<sub>2</sub> was added in the PEEK matrix. Also, the wear rate of the composites decreases by 27 times when 5 volumetric % of Ti<sub>3</sub>SiC<sub>2</sub> was added. In Chapter III, novel self-lubricating Teflon-Ti<sub>3</sub>SiC<sub>2</sub> and Nylon-Ti<sub>3</sub>SiC<sub>2</sub> composites are reported. During self-mating, Ti<sub>3</sub>SiC<sub>2</sub>-Teflon composites showed better performance than Ti<sub>3</sub>SiC<sub>2</sub>-Nylon composites. In the case of friction coefficient, a marginal decrease is observed for Teflon composites but for Nylon-Ti<sub>3</sub>SiC<sub>2</sub> composites, an increase in friction coefficient is observed as the percent content of Ti<sub>3</sub>SiC<sub>2</sub> was increased. However, the wear rate decreased to  $(5 \pm 3) \times 10^{-5} \text{ mm}^3/\text{N.m}$  and  $(1 \pm 1.5) \times 10^{-5} \text{ mm}^3/\text{N.m}$  in Teflon-5%Ti<sub>3</sub>SiC<sub>2</sub> and Teflon-10%Ti<sub>3</sub>SiC<sub>2</sub>, respectively, and thereafter retained a similar value of  $(1.6 \pm 1.6) \times 10^{-5}$  in Teflon-30%Ti<sub>3</sub>SiC<sub>2</sub>. We have observed a decrease in wear rate for Nylon-Ti<sub>3</sub>SiC<sub>2</sub> composites but it is very marginal decrease. In Chapter IV of this thesis, the scope of future studies are discussed.

# CHAPTER I

## INTRODUCTION

### 1.1 MAX Phase

One of the major modern day challenges in engineering is the need of versatile materials to fulfill the demand of rapidly growing technologies. Metals are ideal when we need durability and high performance in extreme environments because of their high damage tolerance and sustainability at high temperature. On the other hand, ceramics are different being elastically rigid, resistant to fatigue and oxidation. For designing ideal high-performance structural materials all these properties are required. To get this versatility in the material researchers have explored a new class of materials named MAX phase [1].

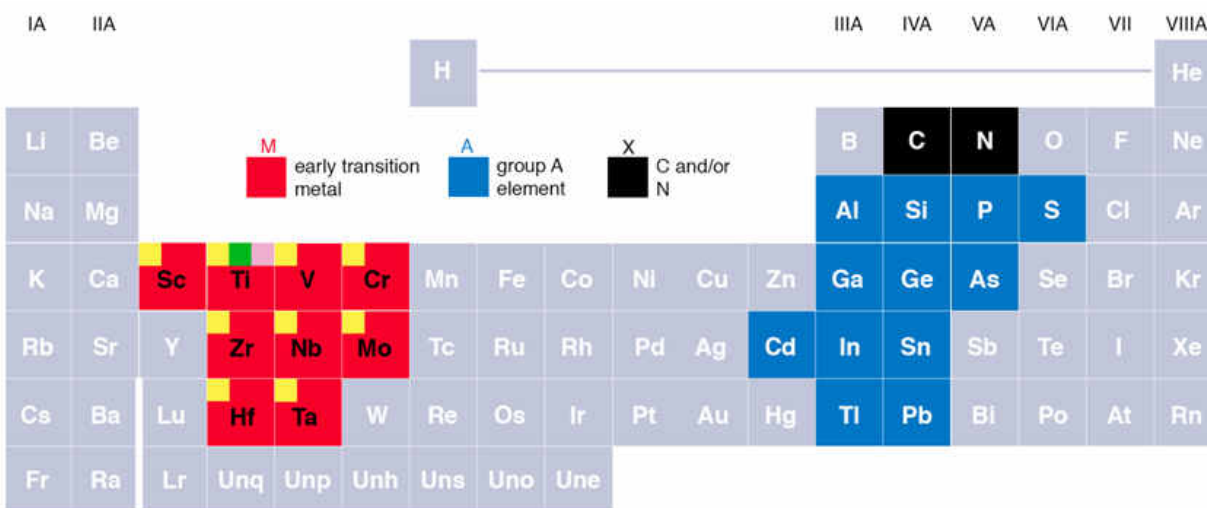


Fig1.1 Possible combination of MAX phases [2]

MAX phases are layered, hexagonal carbides and nitrides with general formula  $M_{n+1}AX_n$  (MAX) where  $n=1-3$ , M stand for the early transition metal, A stands for group-A elements and X are either carbon or nitrogen. Fig 1.1 shows the different combination that can be used to fabricate MAX phases. MAX phases are highly damage tolerant, oxidation resistant at high temperatures, readily machinable and have a Vickers's hardness values of 2-8 GPa [2-6]. MAX phases consist of over 60 different ternary carbides and nitrides. When  $n=1, 2,$  and  $3$  the series of MAX phases are known as 211, 312, and 413, respectively [2]. The unit cell of MAX phases for 3 different series of MAX phases are shown in Fig 1.2. Significant research has been done on MAX phases after Barsoum et al. synthesized MAX phases for the first time incorporating both the properties of metal and ceramic in the mid-1990s [4].

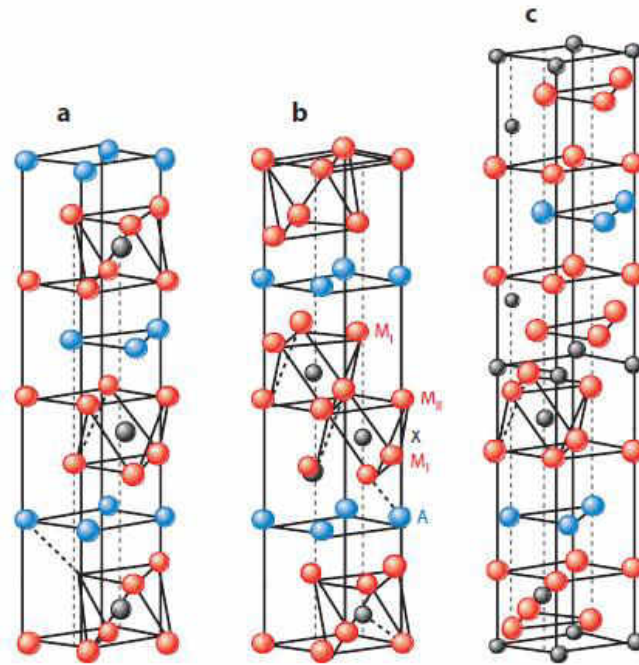


Fig 1.2 Unit Cell for 211(a), 312 (b) and 413 (c) series of MAX phases [2]

The layered structure of MAX phases indicate that it might show solid lubricity which is true as the first ever MAX phase,  $Ti_3SiC_2$ , was felt lubricious [4].

In this research,  $Ti_3SiC_2$  was used as the primary MAX phases; thereafter three more MAX phases ( $V_2AlC$ ,  $Cr_2GaC$  and  $Cr_2AlC$ ) were used.

## 1.2 Background Study of Polymer Matrix Composites

Generally, polymers can be classified into two types, thermoplastic and thermoset. Both thermoset and thermoplastic polymers are mostly used for fabricating polymer matrix composites [7]. In recent years, polymers have become attractive materials for different applications due to their low weights, ease of processing and low cost [7]. Hence there are many attempts to improve the properties of polymers by various reinforcements including fiber reinforcement [8]. Fiber-reinforced polymer matrix composites are important due to their high strength, light weight, and low friction coefficient and now being used in different household works to aerospace applications [7-10]. Carbon fibers are widely used as reinforcements in polymer matrix composites as carbon fibers have the highest modulus of elasticity and strength [10].

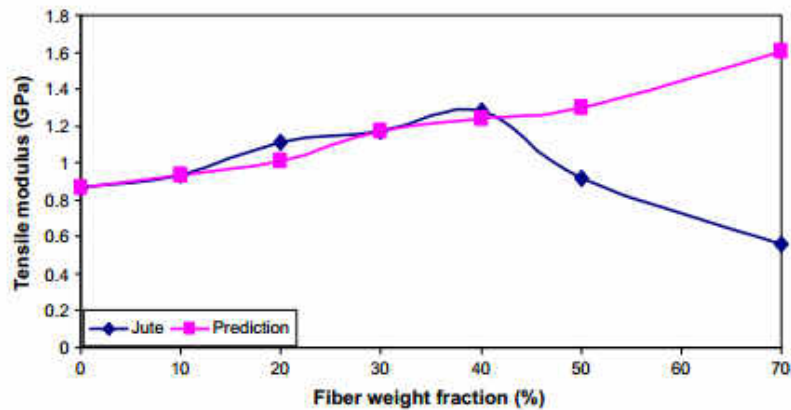


Fig 1.3 Predicted and experimental result of tensile modulus of jute-reinforced PP composites [8]

Currently, natural fibers are being used as an alternative to glass fiber and carbon fiber due to their environmental benefits over other fibers.

The natural fibers are low-cost fibers with low density and high specific properties. These are also nonabrasive and biodegradable [11]. From Fig. 1.3 [8], it was observed that natural fibers can increase the tensile strength of the polymer matrix composite when the weight ratio of the fiber is increased in the polymer matrix up to an optimum value; after that the tensile strength decreased a bit. Also, Emad Omrani et al. [7] found that friction coefficient and wear rate of the polymer matrix composite reinforced with fiber (natural or artificial) is much lower than the original polymer. During the same study, the researchers also found that seed oil palm reinforced polyester composites shows similar wear behavior as woven glass reinforced polyester. Emad Omrani et al. [7] also suggested that natural fiber can replace the glass fiber as a reinforcement for polymer composites. Another group of researchers found that the addition of carbon nanotube and carbon fiber fabric can increase the mechanical strength of the polymer matrix composite [12]. From the background study, it was observed that a lot of work has been done to improve the mechanical and tribological behavior of polymer matrix composite. During this research, the impact of MAX phases as a reinforcement to the polymer matrix composite is studied.

### **1.3 Introduction of MAX Reinforced Polymers (MRPs)**

MAX reinforced polymers (MRPs) are composites made out of polymer matrix where MAX phase is used as the particulate reinforcement. Gupta et al. [2] showed that MAX phases at room temperature shows dual characteristics; in stage one they show low friction coefficient and wear but in stage two they show high friction coefficient and wear. It is because of the formation of third

body abrasion in the later stage (Fig. 1.4). But at high-temperatures MAX phases show low friction coefficient and negligible wear [2].

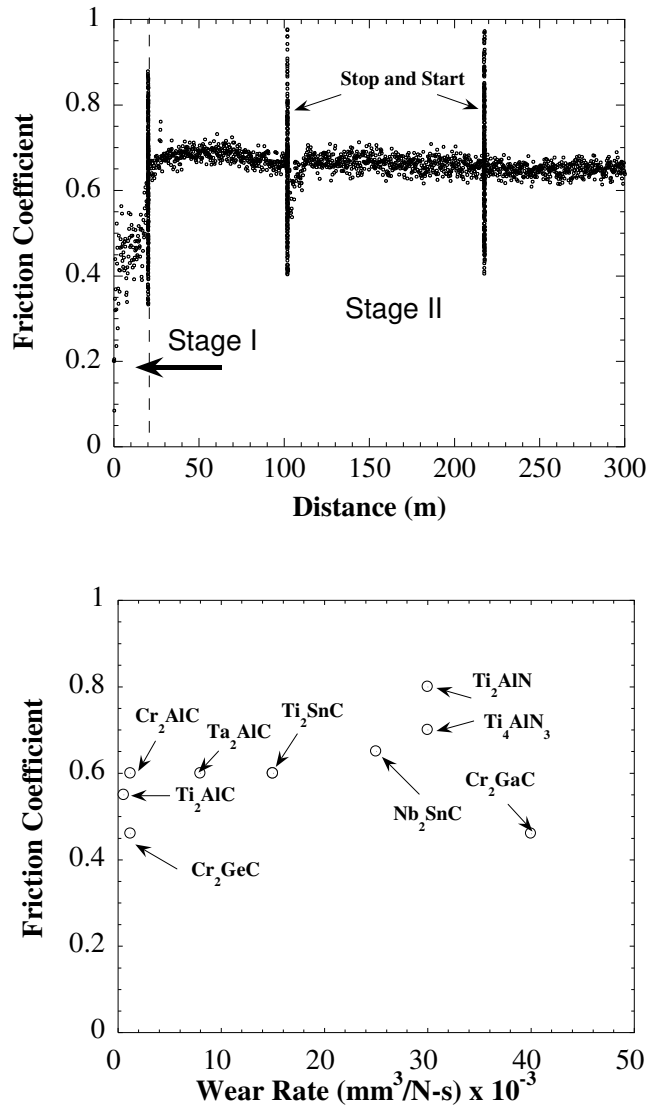


Fig. 1.4 Tribological performance of MAX phases at room temperature [2]

From the study of MRM composites by Gupta et al. [13-17] it is well established that at room temperature MAX phases are an outstanding materials to use as particulate reinforcement. When composites are made of metal matrix and MAX phases are used as a particulate reinforcement it is called max reinforced metal (MRM) [14]. Gupta et al. showed that MAX phases can be used as

a particulate reinforcement to the metal matrix. When MAX phases are used as a particulate reinforcement it usually enhanced the mechanical properties as well as the tribological properties of metal matrix composites [13-16]. Gupta et al. [14] also claimed that the addition of MAX phases in the metal matrix also imparts self-lubricity in the MRM composites. So it is fairly interesting to investigate what happens when MAX phases are introduced into a polymer matrix. Polymers are low-density materials. Polymers and their composites are extensively used in automobile, aerospace, and chemical sectors because of their properties like light weight, excellent strength-to-weight ratios and resistance to corrosion [17]. In general, ceramic particles are added to the polymer matrix as particulate reinforcement to increase the mechanical and tribological behavior of polymer matrix composites [18]. Recently, Gupta et al. claimed that the addition of hard, machinable, conductive and lubricious MAX particles can impart self-lubricity and improve the mechanical and tribological behavior of epoxy matrix composites [18].

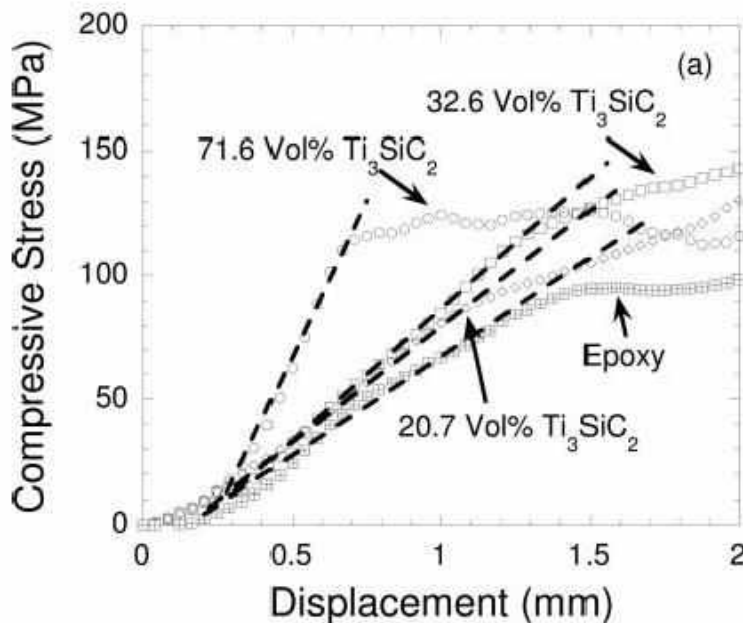


Fig 1.5 Mechanical performance of epoxy- $Ti_3SiC_2$  composites [18]

Fig 1.5 shows that the addition of MAX phases increased the yield strength of the epoxy matrix composites. Also, Fig 1.6 shows the friction coefficient of the MAX-Epoxy composites decreases with the increasing percent content of MAX phase. Also, the wear rate of the MAX-Epoxy composite decreases until a certain percent content of MAX phases in the Epoxy matrix [18]. Unfortunately not many works have been reported in the literature on the design of MAX reinforced polymer matrix composites other than the Epoxy-Ti<sub>3</sub>SiC<sub>2</sub> composites by Gupta et al. [18].

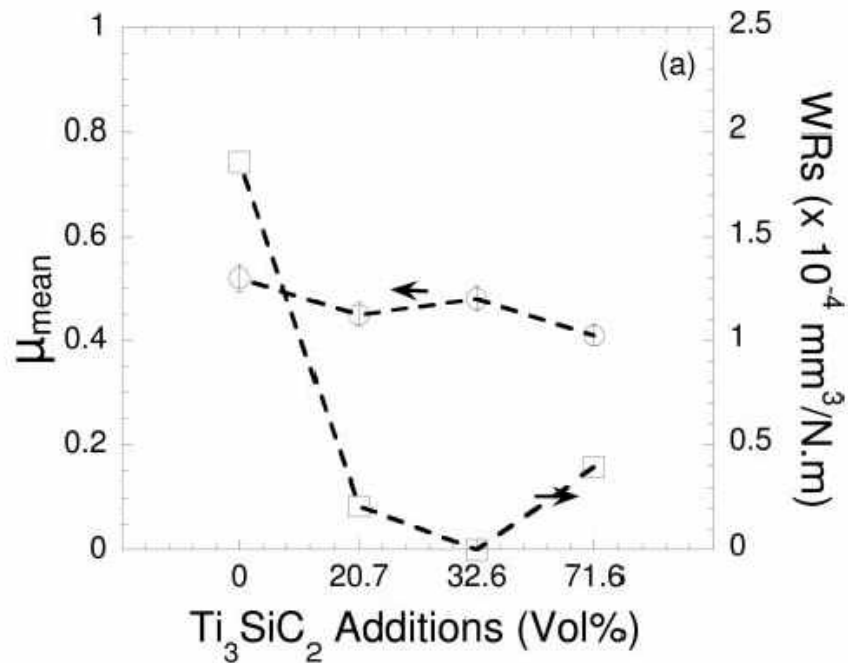


Fig 1.6. Tribological performances of Epoxy-Ti<sub>3</sub>SiC<sub>2</sub> composite against Inconel 718 substrate [18]

During this thesis, a wide range of thermoplastic polymers will be selected to fabricate the MAX reinforced polymers. As a starting point, Ti<sub>3</sub>SiC<sub>2</sub> will be used as the primary MAX phase

to work with; thereafter different MAX phases ( $\text{Cr}_2\text{AlC}$ ,  $\text{V}_2\text{AlC}$  and  $\text{Cr}_2\text{GaC}$ ) will be used to fabricate MAX reinforced polymers. Powders of MAX phases and polymers will be mixed according to the volumetric ratio and then heated to a desired temperature (for example  $450^\circ\text{C}$  for PEEK-based MAX reinforced polymers,  $350^\circ\text{C}$  for Nylon and Teflon based MAX reinforced polymers) at a heating rate of  $5^\circ\text{C}/\text{min}$  will be used to fabricate these composites. After reaching the desired temperature; the samples will be held for 20 minutes at that temperature and then a pressure of 120 MPa will be applied. Thereafter, the sample will be cooled in the environmental air. The hardness of the fabricated sample will be measured by Vickers's hardness tester. Then the sample will be machined into a 3 mm cubic shape to do the tribology test and compressive test. 5 KN load cell will be used for testing the compressive strength of the MAX reinforced polymers composites. The CSM tribometer will be used for the tribology study of these composites. All the tribology studies will be performed by a tab on disc method at 5 N load and 31 cm/s linear speed. SEM and EDS study will be done to study the surface of the composites and the micro constituent of the tribo films. Gupta et al. [2] had proposed a method of classifying tribofilms. Tribofilms are classified according to the face contributing to the formation of tribofilms. Details of the proposed method is listed in the Table 1.1.

It is expected the MAX reinforced polymers composite will show a higher hardness than the original polymer matrix due to the addition of harder MAX phases. It is also expected that the porosity of the samples will increase with the increase of percentage content of MAX phase. The MAX reinforced polymers are also expected to have higher mechanical strength than the polymer in pure form. But the most important anticipation of the study is that there will be a significant tribological improvement in MAX reinforced polymers than original polymer matrix at self-

ming. As it is well-known that MAX phase can show self-lubricity, the researchers expect that MAX phase will impart lubricity in the MAX reinforced polymers composite thus help to decrease the friction coefficient and wear rate of the MAX reinforced polymers composites.

Table 1.1 A novel method of classifying tribofilms [2]

Source of tribofilms	Tribofilms	Temperature	Characteristics
MAX phase	Ia	Ambient	Barely visible to naked eyes and iridescent layers or spots observed by optical microscopy
	Ib		Powdery and abrasive third body
	Ic		Patchy lubricious tribofilms on the surface
	Id	550 °C	Completely or partially tribooxidized lubricious and/or antiwear tribooxides
Inconel 718	IIa		“Glazed” lubricious oxides
	IIb		Glazed and multiple layered lubricious oxides
Both MAX or MAX/Ag and SA’s surface	IIIa	Ambient	barely visible to naked eyes and amorphous thin layers over each tribosurface by SEM
	IIIb	Thermal cycling	Glazed and multiple layered
MAX/Ag	IVa	Ambient	Lubricious and no phase separation observed in the microscale
	IVb	550 °C	Phase Separated

It is also expected that a lubricious tribofilm will form in the interface of contacting surfaces which helps to reduce the friction and wear. These novel materials can be used for different multi-functional applications, such as in bearing materials.

## CHAPTER II

### SYNTHESIS AND TRIBOLOGICAL BEHAVIOR OF NOVEL WEAR RESISTANT PEEK-Ti<sub>3</sub>SiC<sub>2</sub> COMPOSITES

#### 2.1 Introduction

Poly ether ether ketone (PEEK) is a promising material for numerous engineering applications, such as, aerospace, military, nuclear plants, chemical process equipment and oil-well applications as it is bestowed with excellent properties like abrasion resistance, low water absorption, excellent chemical and hydrolysis resistance, durability in steam or high pressure environments without any detrimental effects on properties, very low flammability, and low emissions of smoke and toxic gas during combustion [1-4]. One of the successful method of further improving the properties of high performance polymers like PEEK further is by using fillers like graphene [5], WS<sub>2</sub> [5], carbon nanotube [5, 6], Al<sub>2</sub>O<sub>3</sub> [7, 8], SiO<sub>2</sub> [8], Si<sub>3</sub>N<sub>4</sub> [9], SiC [10, 11], glass Fibers [12], PTFE [13], h-BN [14], and CuS [15]. Table 2.1 summarizes the tribological behavior of PEEK composites against metal counterparts. Interestingly, similar studies for self-mating are lacking [16]. High performance polymers based polymer-on-polymer devices can have various applications; for example, Scholes and Unsworth [16] have envisioned that all-polymer combinations may provide engineers with new approaches for designing novel medical devices. It is expected that novel high performance devices can be designed by adding hard, machinable, conductive, oxidation resistant, and lubricous particles in a polymer matrix. MAX phases are excellent candidate as filler materials.

Recently, Gupta et al. [23-24] reported for the first time the fabrication of novel MAX-Polymer composites by incorporating  $\text{Ti}_3\text{SiC}_2$  particulates (MAX Phase) in epoxy and UHMWPE (Ultra High Molecular Weight Polyethylene) matrix. These composites showed enhanced mechanical and tribological performance as compared to the base polymeric matrix. More particularly, UHMWPE- $\text{Ti}_3\text{SiC}_2$  composites showed excellent tribological behavior during self-mating, for example, the  $\mu_{\text{mean}}$  decreased from  $\sim 0.54$  in UHMWPE to  $\sim 0.15$  in 35 vol%  $\text{Ti}_3\text{SiC}_2$ -UHMWPE [24]. In this Chapter II, we report for the first time the synthesis and characterization of  $\text{Ti}_3\text{SiC}_2$ -PEEK composites. This study was already published in the Proceedings of the Institution of Mechanical Engineers, "Synthesis and Tribological Behavior of Novel Wear Resistant PEEK- $\text{Ti}_3\text{SiC}_2$  composites", S. Ghosh, R. Dunnigan and S. Gupta, Journal of Engineering Tribology, 2016, DOI: 10.1177/1350650116648868.

## 2.1 Experimental Methods

PEEK (average particle size 20  $\mu\text{m}$ , Goodfellow Cambridge Limited, Huntingdon, England) and  $\text{Ti}_3\text{SiC}_2$  (-325 mesh, 40-50  $\mu\text{m}$ , Kanthal, Hallstahammar, Sweden) powders were used to fabricate composites. During this study four different compositions were designed by reinforcing PEEK matrix with 5 vol% (PEEK-5% $\text{Ti}_3\text{SiC}_2$ ), 10 vol% (PEEK-10% $\text{Ti}_3\text{SiC}_2$ ), 20 vol% (PEEK-20% $\text{Ti}_3\text{SiC}_2$ ), and 30 vol%  $\text{Ti}_3\text{SiC}_2$  (PEEK-30% $\text{Ti}_3\text{SiC}_2$ ), respectively. All the samples were produced by hot pressing (HP). The required amount of powders were dry ball milled (8000 M mixer Mill, SPEX SamplePrep, Metuchen, NJ) for 30 minutes. All the powders were then poured in a die (EQ-Die-12D, MTI Corporation, Richmond, CA). The compositions were then sintered by hot pressing (HP) (Model EQ-HP-6T, MTI Corporation, Richmond, CA) in atmospheric air.

Table 2.1: Summary of tribological behavior of PEEK samples

Surface	Countersurface	Filler	Conditions	WR (mm <sup>3</sup> /N.m)	Friction	Ref.
100Cr6 cylinder	PEEK	No Fillers	Linear reciprocating, 1 MPa, and 0.05 m/s	3 x 10 <sup>-6</sup>	0.6	5
		WS <sub>2</sub> (fullerene, 2 wt%)		2 x 10 <sup>-6</sup>	0.45	
		WS <sub>2</sub> (needle like particle, 2 wt%)		1 x 10 <sup>-6</sup>	0.75	
		CNT (multi-wall carbon nanotubes, 2 wt%)		3 x 10 <sup>-6</sup>	0.45	
		GNP (Graphene, 2 wt%)		9 x 10 <sup>-6</sup>	0.6	
AISI 1045 Steel	PEEK	No Fillers	Block-on-Ring, 196 N, and 0.42 ms <sup>-1</sup>	13 x 10 <sup>-6</sup>	0.33	7
		PTFE (10 wt%)		5 x 10 <sup>-6</sup>	0.25	
		Al <sub>2</sub> O <sub>3</sub> (500 nm, 5 wt%)		7.5 x 10 <sup>-6</sup>	0.33	
		Al <sub>2</sub> O <sub>3</sub> (500 nm, 5 wt%) and PTFE (10 wt%)		10 x 10 <sup>-6</sup>	0.27	
Plain Carbon	PEEK	No Fillers	Ring-on-Block, 196 N, and 0.42 ms <sup>-1</sup>	7 x 10 <sup>-6</sup>	0.375	9
		Si <sub>3</sub> N <sub>4</sub> (<50 nm, 8 wt%)		1 x 10 <sup>-6</sup>	0.25	
Plain Carbon	PEEK	No Fillers		7 x 10 <sup>-6</sup>	0.275	10
		SiC (<100 nm, 10 wt%)		4 x 10 <sup>-6</sup>	0.21	
100C6	PEEK	No Fillers	Ball-on-disc, 5 N, and 0.5 m/s	50 x 10 <sup>-6</sup>	0.3	11
		SiC (2-3 μm, 7 wt%)		20 x 10 <sup>-6</sup>	0.4	
AISI 1045 Steel	PEEK	No Fillers	Pin-on-disc, 8 MPa, and 0.25 m/s	5 x 10 <sup>-6</sup>	0.21	12
		30 wt% Carbon Fibers		0.6 x 10 <sup>-6</sup>	0.18	
		30 wt% Glass Fibers		0.9 x 10 <sup>-6</sup>	0.25	
AISI 304	PEEK	No Fillers	Linear reciprocating, 6.25 MPa, 50.8 mm/s	5 x 10 <sup>-3</sup>	0.13	13
		32 wt% PTFE		2 x 10 <sup>-9</sup>	0.115	
		50 wt% PTFE		2 x 10 <sup>-8</sup>	0.11	
Hardened Steel	PEEK	No Fillers	Ball-on-Disc, 5 N, 0.1 m/s,	40 x 10 <sup>-6</sup>	0.24	14
		h-BN (0.5 μm, 8 wt%)		30 x 10 <sup>-6</sup>	0.25	
PEEK-OPTIMA	PEEK-OPTIMA	No Fillers	Multidirectional pin-on-plate, 2 MPa, 25 mm stroke length, 2-5 million cycles, 1 Hz frequency	4.5 x 10 <sup>-6</sup>	NA	16
CFR-PEEK (PAN)	CFR-PEEK (PAN)	Carbon Fibers		0.3 x 10 <sup>-6</sup>	NA	
CFR-PEEK (Pitch)	CFR-PEEK (Pitch)	Carbon Fibers		0.9 x 10 <sup>-6</sup>	NA	

During HP, samples were heated at 5° C/min to 450° C, then they were held at 450° C for 20 min, thereafter a uniaxial compressive stress of ~120 MPa was applied for 5 minutes, and the furnace was slowly cooled to ambient temperature. The hot pressed samples were then demolded from the die, and used for further characterization. For comparison, pristine PEEK compacts were also prepared by following the above-mentioned procedure.

Samples were mounted on aluminum mounts and coated with Au/Pd using a Balzers SCD 030 sputter coater (BAL-TEC RMC, Tucson, AZ). SE (Secondary Electron) and BSE (Back Scattered Electron) images were obtained by using a JEOL JSM-6490LV Scanning Electron Microscope (JEOL USA, Inc., Peabody, Massachusetts). X-ray information was obtained via a Thermo Nanotracer Energy Dispersive X-ray detector with NSS-300e acquisition. In this Chapter II, the researcher will use a procedure outlined by Gupta et al. [21, 22] to characterize the chemical composition of the tribosurfaces. Briefly, two asterisks will be used to designate a chemically uniform region at the micron level as quantified by Energy Dispersive Spectroscopy (EDS). These regions will be designated as \*microconstituent\* to emphasize that these areas are not necessarily single phases. The presence of C in these tribofilms is shown by adding {C<sub>x</sub>} in the composition. Prior to hardness testing all composites were polished ( $R_a < 1\ \mu\text{m}$ ) and then tested on a Vicker's micro-hardness indenter (Mitutoyo HM-112, Mitutoyo Corporation, Aurora, IL). Vicker's hardness was measured by loading the samples at 2.9 N for 15 s. An average of five readings for each composite was measured and is reported in this text.

All the tribology studies were then performed by a tab-on-disc tribometer (CSM Instruments SA, Peseux, Switzerland) at 5 N (~0.3 MPa), 31 cm/s linear speed, 5000 m sliding distance, ~9 mm track radius, and ~264 min cycling time. The HP samples were cut into tabs with dimensions

of ~4 mm x ~4 mm (cross-section) x ~3 mm (thickness). The HP samples were also used as disks (substrates). For each composition, a set of three experiments was performed. A surface profilometer (Surfcom 480A, Tokyo Seimitsu Co. Ltd., Japan) was used to measure surface finish of all the samples after polishing. Table 2.2 summarizes the surface finish of all the samples before and after tribology testing. Three experimental studies were performed for each composition to determine the surface roughness. The data analysis was performed by calculating an average of friction coefficient ( $\mu$ ) readings during a single experiment; thereafter, an average of three mean values from three experiments was calculated and reported in the text as  $\mu_{\text{mean}}$ . The masses of the tabs and disks were measured before and after the testing by a weighing scale (XA 83/220/2X, Radweg, Radom, Poland). The specific wear rate (WR) was calculated from:

$$WR = (m_i - m_f)/(\rho \cdot N \cdot d) \text{ -----(I)}$$

where,  $m_i$  is the initial mass,  $m_f$  is the final mass,  $\rho$  is density of the composite,  $N$  is the applied load, and  $d$  is the total distance traversed by the static partner during the tribology testing. In the text, total WR of both the tabs and disks is reported and will be referred to as WR.

Table 2.2: The surface roughness before and after the tribological testing

Tribocouples	Substrate ( $R_a$ ) ( $\mu\text{m}$ )		Tab ( $R_a$ ) ( $\mu\text{m}$ )	
	Before	After	Before	After
PEEK	0.30±0.01	0.20±0.04	0.19±0.01	0.25±0.01
PEEK-5%312Si	0.17±0.04	0.23±0.02	0.15±0.02	0.18±0.01
PEEK-10%312Si	0.20±0.07	0.26±0.02	0.17±0.03	0.26±0.04
PEEK-20%312Si	0.63±0.14	0.24±0.12	0.32±0.06	0.23±0.06
PEEK-30%312Si	1.37±0.37	2.06±0.51	0.97±0.15	2.06±0.51

## 2.3 Results and Discussion

### 2.3.1 Investigation of the Microstructures

Figure 2.1 shows the SEM micrographs of  $\text{Ti}_3\text{SiC}_2$ - PEEK composites.  $\text{Ti}_3\text{SiC}_2$  particulates are well-dispersed in the PEEK matrix when the concentration of  $\text{Ti}_3\text{SiC}_2$  particulates is ~5 and 10 vol%  $\text{Ti}_3\text{SiC}_2$ , respectively (Figs. 2.1a-d). However, in PEEK-20% $\text{Ti}_3\text{SiC}_2$  (Figs. 2.1e-f) and PEEK-30% $\text{Ti}_3\text{SiC}_2$  (Figs. 2.1 g-h) some signs of agglomeration and porosities in the microstructure were observed. Figure 2.2a plots the variation of porosity (Y1 axis) and hardness (Y2 axis) versus PEEK concentration. Clearly, as the concentration of  $\text{Ti}_3\text{SiC}_2$  particulates was increased in the PEEK matrix, the porosity of the sample was increased. This observation corroborates the microstructural features observed by SEM analysis (Fig. 2.1).

In earlier studies, we have observed similar behavior where the addition of stiffer  $\text{Ti}_3\text{SiC}_2$  particulates make the densification of these composites difficult [25, 26]. Comparatively, the hardness of PEEK sample was ~141 MPa, it increased to ~169 MPa in PEEK-5% $\text{Ti}_3\text{SiC}_2$ ; thereafter, it decreased gradually to ~152 MPa and ~123 MPa in PEEK-80% $\text{Ti}_3\text{SiC}_2$  and PEEK-70% $\text{Ti}_3\text{SiC}_2$ , respectively (Fig. 2.2a). The increase in porosity of the composites with the concentration of  $\text{Ti}_3\text{SiC}_2$  is responsible for the lower hardness of the composites at higher concentration of  $\text{Ti}_3\text{SiC}_2$  particulates in the PEEK matrix.

### 2.3.2 Tribological Behavior

Figure 2.2b shows  $\mu$  versus distance profiles of different  $\text{Ti}_3\text{SiC}_2$ -PEEK composites during self-mating. In all cases,  $\mu$  was stable during the tribological testing. The PEEK had a  $\mu_{\text{mean}}$  of ~0.19, and it gradually decreased to ~0.14 in PEEK-10% $\text{Ti}_3\text{SiC}_2$ ; thereafter, it increased to ~0.21 in PEEK-20% $\text{Ti}_3\text{SiC}_2$ , and retained similar value in PEEK-30% $\text{Ti}_3\text{SiC}_2$  sample (Fig. 2.2c).

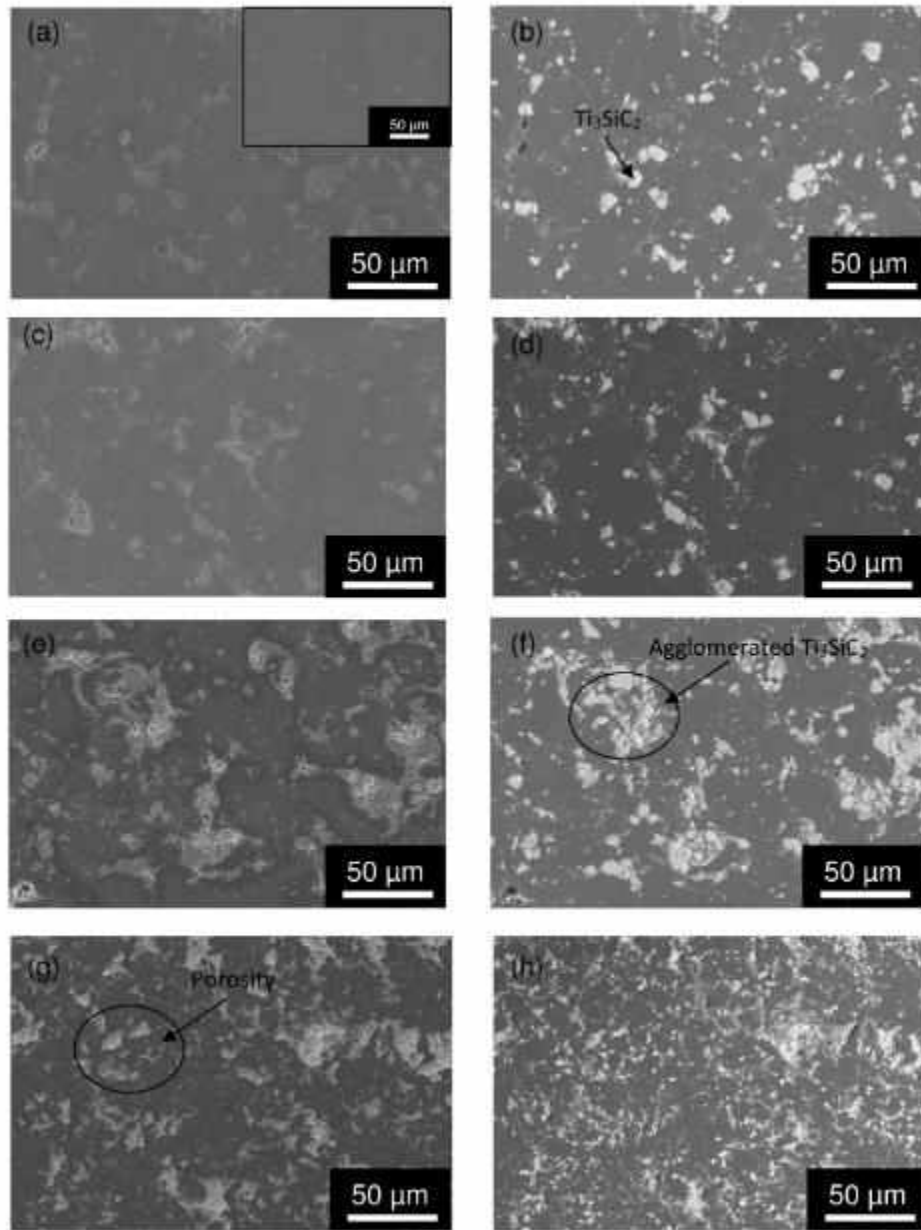


Figure 2.1: SEM SE image of the polished surface of (a) PEEK-5% $\text{Ti}_3\text{SiC}_2$  PEEK (inset shows the SEM SE polished surface of PEEK) surface, (b) BSE image of the same region, (c) PEEK-10% $\text{Ti}_3\text{SiC}_2$  PEEK, (d) BSE image of the same region, (e) PEEK-20% $\text{Ti}_3\text{SiC}_2$  PEEK, (f) BSE image of the same region, (g) PEEK-30% $\text{Ti}_3\text{SiC}_2$  PEEK, and (h) BSE image of the same region.

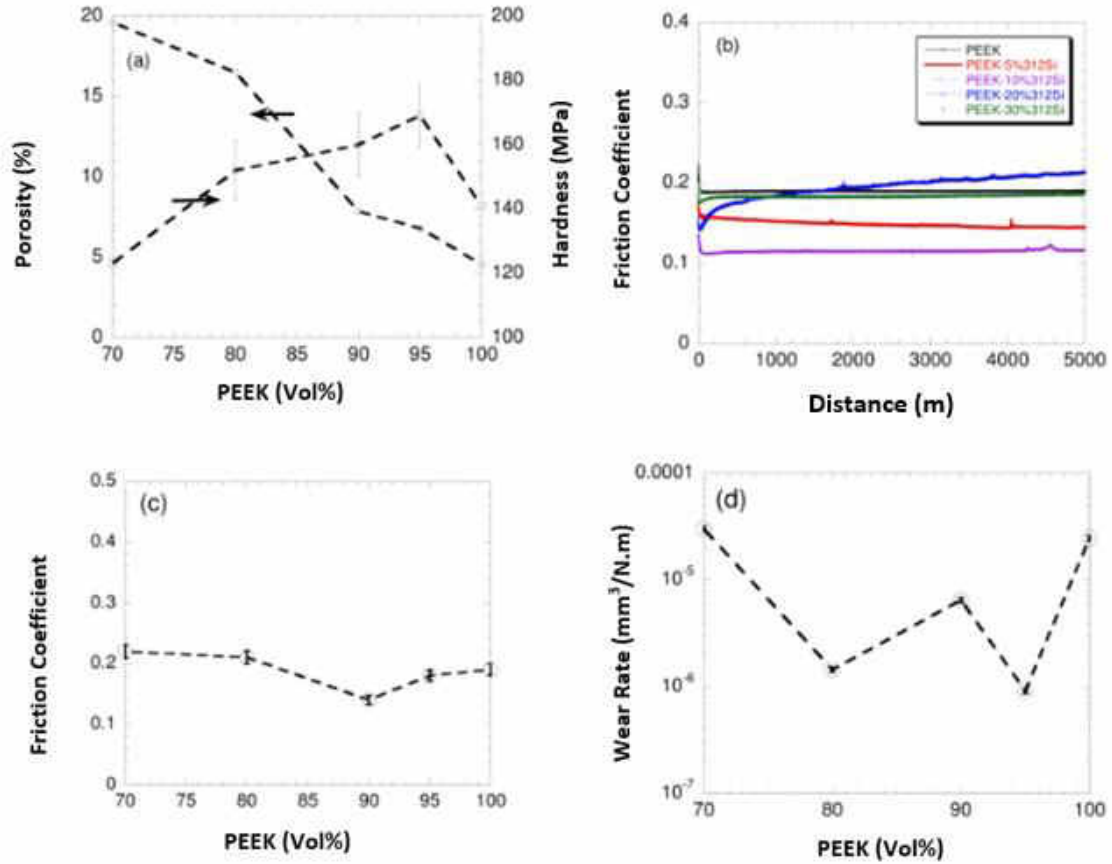


Figure 2.2: Plot of (a) porosity (Y1 axis) and Hardness (Y2 axis), (b) friction coefficient ( $\mu$ ) versus distance, (c) mean friction coefficient ( $\mu_{\text{mean}}$ ), and (d) total WR versus PEEK concentration (vol%) of different PEEK-Ti<sub>3</sub>SiC<sub>2</sub> composites.

The concomitant WR of PEEK was  $\sim 2.4 \times 10^{-5} \text{ mm}^3/\text{N.m}$  (Fig. 2d), it decreased sharply to  $\sim 9.1 \times 10^{-7} \text{ mm}^3/\text{N.m}$  in PEEK-5%Ti<sub>3</sub>SiC<sub>2</sub>; thereafter it increased to  $\sim 6.5 \times 10^{-6} \text{ mm}^3/\text{N.m}$ ,  $\sim 1.4 \times 10^{-6} \text{ mm}^3/\text{N.m}$ , and  $\sim 3.0 \times 10^{-5} \text{ mm}^3/\text{N.m}$  in PEEK-10%Ti<sub>3</sub>SiC<sub>2</sub>, PEEK-20%Ti<sub>3</sub>SiC<sub>2</sub>, and PEEK-30%Ti<sub>3</sub>SiC<sub>2</sub> samples, respectively. Several factors like porosity, phase boundary decohesion between Ti<sub>3</sub>SiC<sub>2</sub>

particulates and polymer matrix can account for this behavior. More detailed studies are needed to understand the effect of each of these parameters.

### 2.3.3 Investigation of Tribosurfaces and Potential Mechanism

Figure 2.3 shows the SEM micrographs of the PEEK (Fig. 2.3a) and PEEK-20% $\text{Ti}_3\text{SiC}_2$  (Figs. 2.3b-d) after the tribology testing. The PEEK surface (Fig. 2.3a) was covered with adhesive wear marks whereas the PEEK-20% $\text{Ti}_3\text{SiC}_2$  surface did not show any wear marks in SE, but in BSE minor wear marks were visible. Clearly, there was negligible mass transfer between the tribosurfaces although mild oxidation of  $\text{Ti}_3\text{SiC}_2$  particulates were observed. For example, a microconstituent region (1) had a chemistry of  $*(\text{Ti}_{0.8}\text{Si}_{0.2})\text{O}_{0.03}\{\text{Cx}\}*$  (Fig. 2.3d). The surface roughness of the samples (tabs and discs) also retained similar values before and after the testing process (Table 2.2). Gupta and Barsoum [21] had proposed a classification system for tribofilms. They designated Type III tribofilms as those tribofilms which are formed by triboreactions at both the counter and MAX or MAX based composite surfaces. More particularly, Type IIIa can be classified as those tribofilms which are barely visible to naked eyes and for amorphous thin layers over each tribosurface by SEM analysis. Thus, by using the classification proposed by Gupta and Barsoum [21], the tribofilms formed on the PEEK-20% $\text{Ti}_3\text{SiC}_2$  surface can be classified as Type IIIa. Due to the complexity of the tribological testing, it is fairly difficult to have a direct comparison of the results obtained during this study with other PEEK-based particulate composites, especially during self-mating [16]. However, based on the results summarized in Table 2.1, for example, CFR-PEEK showed an improvement of 1.5 times in WR as compared to PEEK samples during self-mating whereas PEEK-5% $\text{Ti}_3\text{SiC}_2$  tribocouple showed 27 times more wear resistance than PEEK

tribocouples. Clearly, PEEK-Ti<sub>3</sub>SiC<sub>2</sub> composites are promising materials for tribological applications.

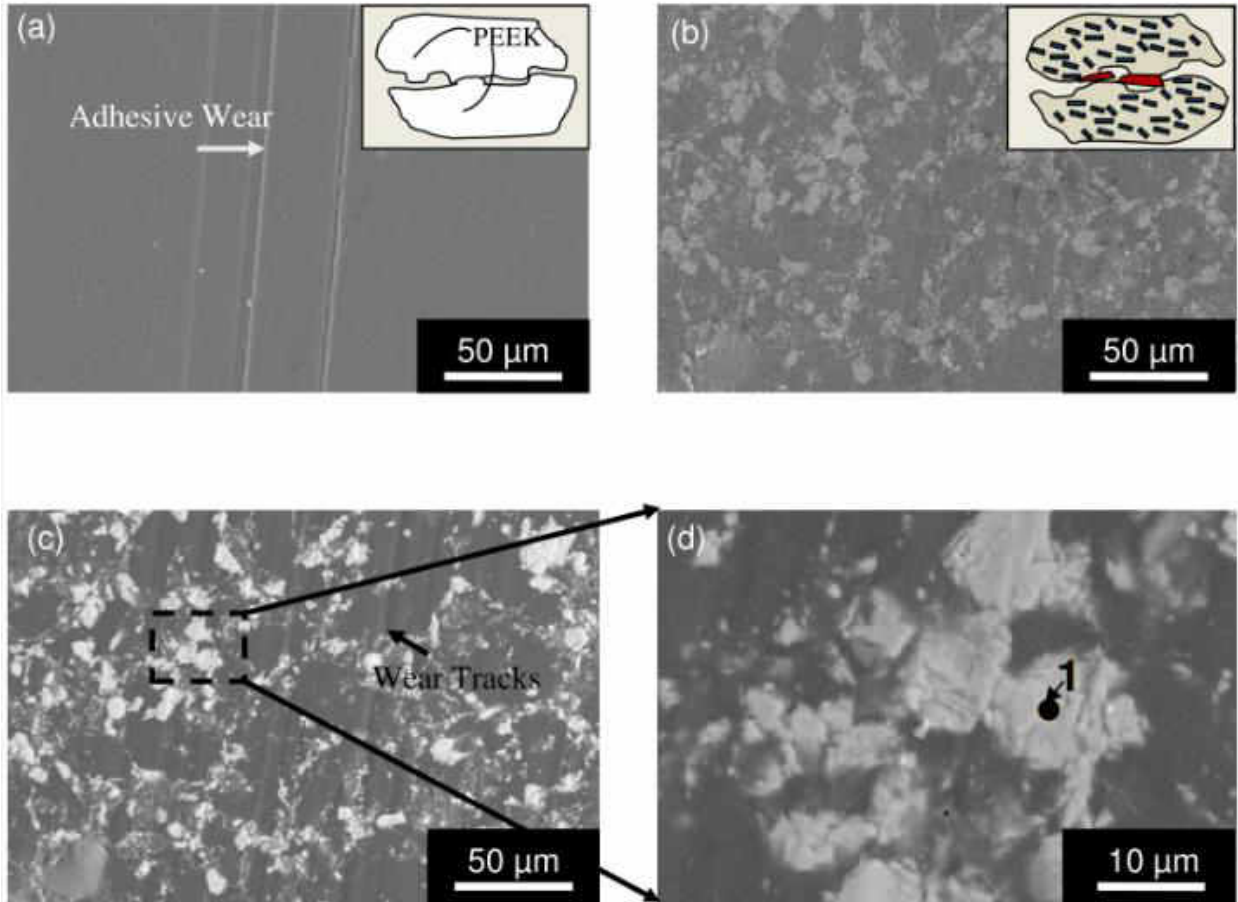


Figure 2.3: SEM SE images of (a) PEEK (inset shows the schematics of adhesive wear), (b) PEEK-20%Ti<sub>3</sub>SiC<sub>2</sub> (inset show the schematics of lubricious and WR Type IIIa tribofilm), (c) BSE image of the same region, and (d) higher magnification of the encircled region in (c) after tribology testing (the chemistry of micro-constituent region 1 is  $*(Ti_{0.8}Si_{0.2})O_{0.03}\{Cx\}*$

## 2.4 Conclusions

1. During self-mating, Ti<sub>3</sub>SiC<sub>2</sub>-PEEK showed better solid lubrication behavior than PEEK; for example, as the Ti<sub>3</sub>SiC<sub>2</sub> content in PEEK was increased from 0 to 35 vol%, the  $\mu_{\text{mean}}$  decreased

from ~0.19 to ~0.14 in PEEK-10%312Si, thereafter, it increased to ~0.21 in PEEK-20%312Si and PEEK-30%312Si, respectively.

2. PEEK-5%312Si tribocouple showed the lowest wear rate, and was 27 times more wear resistant than PEEK tribocouples.

3. By using the tribofilm classification proposed by Gupta and Barsoum [21], the tribofilms formed on PEEK-20%312Si surfaces were classified as Type IIIa.

## CHAPTER III

### NOVEL SELF LUBRICATING TEFLON-Ti<sub>3</sub>SiC<sub>2</sub> and NYLON-Ti<sub>3</sub>SiC<sub>2</sub>

#### 3.1 Introduction

Solid lubrication can be attractive due to a variety of reasons like simplicity, cleanliness, low expense, quiet operation, low maintenance, low outgassing and high temperature capability [1]. A low wear solid lubricant is needed for either (a) maintaining long life, or (b) maintaining proper kinematics. Very few materials, however, exhibit low friction and low wear, so the designer is forced to add cost and complexity to accommodate one or the other [1]. Polymers filled with inorganic particulates have emerged as potential materials for solid lubrication applications in polymers, for example, in Teflon [2-10] and Nylon [11-14] based polymeric systems. Tables 3.1 and 3.2 summarize the tribological behavior of different Teflon and Nylon based composites. Recently, Gupta et al. [21-23] reported the fabrication of novel MAX-Polymer composites (MAXPOLs) by incorporating Ti<sub>3</sub>SiC<sub>2</sub> particulates (MAX Phase) in epoxy, and UHMWPE (Ultra High Molecular Weight Polyethylene). In Chapter II, Polyether ether Ketone (PEEK) composites with Ti<sub>3</sub>SiC<sub>2</sub> composites has been discussed. These composites showed enhanced mechanical and tribological performance as compared to the base polymeric matrix. More particularly, UHMWPE-Ti<sub>3</sub>SiC<sub>2</sub> composites showed excellent tribological behavior during self-mating, for example, the  $\mu_{\text{mean}}$  decreased from ~0.54 in UHMWPE to ~0.15 in 35 vol% Ti<sub>3</sub>SiC<sub>2</sub>-UHMWPE.

Table 3.1 Summary of WR and friction coefficient of different PTFE-based tribocouples

Surface	Countersurface	Filler	Conditions	WR (mm <sup>3</sup> /N.m)	Friction	Ref.
PTFE	Stainless Steel	0 vol% ZnO nanoparticles	Ring-on-Block, 200 N, 0.431 m/s	0.001	0.2	2
PTFE	Stainless Steel	5 vol% nanoparticles		8.3E-05	0.21	
PTFE	Stainless Steel	10 vol% nanoparticles		1.9E-05	0.2	
PTFE	Stainless Steel	20 vol% nanoparticles		1.9E-05	0.21	
PTFE	Stainless Steel	30 vol% nanoparticles		3.6E-05	0.21	
PTFE	Steel	0 wt% Ultrafine Diamond	Ring-on-Block, 200 N, 0.42 m/s	0.00062	0.22	3
PTFE	Steel	5 wt%		0.00004	0.2	
PTFE	Steel	10 wt%		0.000026	0.22	
PTFE	Chromium Steel	0 wt% n-MoS <sub>2</sub>	Shaft-Partial Bearing, 0.5 MPa, 50 cm/s	0.0007	0.26	4
PTFE	Chromium Steel	1 wt% n-MoS <sub>2</sub>		0.0002	0.21	
PTFE	Stainless Steel	0 vol% CNT	Ring-on-Disk, 200 N, 200 r/mm	0.0008	0.205	5
PTFE	Stainless Steel	5 vol% CNT		0.000009	0.1875	
PTFE	Stainless Steel	10 vol% CNT		0.000003	0.185	
PTFE	Stainless Steel	20 vol% CNT		0.000002	0.175	
PTFE	Stainless Steel	0 vol% B <sub>2</sub> O <sub>3</sub>	Pin-on-Disk 312 N, 0.025 m/s	0.001	-	6
PTFE	Stainless Steel	5 vol% B <sub>2</sub> O <sub>3</sub>		0.0006	-	
PTFE	Stainless Steel	25 vol% B <sub>2</sub> O <sub>3</sub>		0.00001	-	
PTFE	Stainless Steel	0 wt% Al <sub>2</sub> O <sub>3</sub>	Pin-on-Disk, 260 N, 50 mm/s	0.00035	0.15	7
PTFE	Stainless Steel	4 wt% Al <sub>2</sub> O <sub>3</sub> (38 nm)		0.00002	0.22	
PTFE	Stainless Steel	8 wt% Al <sub>2</sub> O <sub>3</sub> (38 nm)		0.00001	0.21	
PTFE	Stainless Steel	20 wt% Al <sub>2</sub> O <sub>3</sub> (38 nm)		0.0000012	0.19	
PTFE	304 Stainless Steel	0 wt% Additions	Pin-on-Disk, 3.1 MPa, 0.01 m/s	0.0007	0.18	8
PTFE	305 Stainless Steel	5 wt% 20 μm Al <sub>2</sub> O <sub>3</sub>		0.00001	0.18	
PTFE	306 Stainless Steel	5 wt% 40 nm Al <sub>2</sub> O <sub>3</sub>		0.0000001	0.19	
PTFE	Stainless Steel	1 wt% Al <sub>2</sub> O <sub>3</sub> (80 nm) (99% alpha)	Pin-on-Disk, 250 N, 50.8 mm/s	0.0000002	0.23	9
PTFE	Stainless Steel	2 wt% Al <sub>2</sub> O <sub>3</sub> (80 nm) (99% alpha)		0.0000003	0.27	
PTFE	Stainless Steel	5 wt% Al <sub>2</sub> O <sub>3</sub> (80 nm) (99% alpha)		0.00000013	0.18	
PTFE	Stainless Steel	10 wt% Al <sub>2</sub> O <sub>3</sub> (80 nm) (99% alpha)		0.0000002	0.3	
PTFE	PTFE	No Fillers	Pin-on-Disk, 2 N, 0.2 m/s	0.0014	0.3	24
PTFE	PTFE	No Fillers	Block-on-Disk, 5 N, 50 cm/s	0.0007	0.27	This study
PTFE	PTFE	5 vol% Ti <sub>3</sub> SiC <sub>2</sub>		0.00005	0.22	
PTFE	PTFE	10 vol% Ti <sub>3</sub> SiC <sub>2</sub>		0.00001	0.25	
PTFE	PTFE	20 vol% Ti <sub>3</sub> SiC <sub>2</sub>		0.000015	0.23	
PTFE	PTFE	30 vol% Ti <sub>3</sub> SiC <sub>2</sub>		0.000016	0.25	

Table 3.2 Summary of WR and friction coefficient of different Nylon-based tribocouples

Surface	Countersurface	Filler	Conditions	WR (mm <sup>3</sup> /N.m)	Friction	Ref.
Nylon 1010	Steel Ring	0 wt% ZnO Particles (50 μm diameter)	Block-on-Ring, 100 N, 0.42 m/s	0.0064	0.3	11
Nylon 1010	Steel Ring	5 wt% ZnO Particles (50 μm diameter)		0.0064	0.44	
Nylon 1010	Steel Ring	10 wt% ZnO Particle (50 μm diameter)		0.0047	0.43	
Nylon 1010	Steel Ring	15 wt% ZnO Particles (50 μm diameter)		0.0064	0.43	
Nylon 1010	Steel Ring	20 wt% ZnO Particles (50 μm diameter)		0.006	0.43	
Nylon 1010	Steel Ring	5 wt% ZnO Whisker (25 μm diameter)		0.0063	0.4	
Nylon 1010	Steel Ring	10 wt% ZnO Whisker (25 μm diameter)		0.006	0.43	
Nylon 1010	Steel Ring	15 wt% ZnO Whisker (25 μm diameter)		0.0055	0.45	
Nylon 1010	Steel Ring	20 wt% ZnO Whisker (25 μm diameter)		0.0035	0.43	
Nylon 6	Chromium Steel	0 wt% Glass Fiber		Ball-on-Disk, 40 N, 200 rpm	0.000028	
Nylon 6	Chromium Steel	15 wt% Glass Fiber	0.000016		0.21	
Nylon 6	Chromium Steel	0 wt% Addition	Pin-on-Disk, 5 N, 477 rpm	NA	0.1	13
Nylon 6	Chromium Steel	1 wt% IF (Inorganic Fullerene) -WS <sub>2</sub> nanoparticles		NA	0.075	
PA6 (80 wt%) /PPS (20 wt%)	Chromium Steel	0 wt% Addition	Ball-on-Disk, 15 N, 1000 rpm	0.000055	0.4	14
PA6 (80 wt%) /PPS (20 wt%)	Chromium Steel	5 wt% Carbon Fibers (300 mesh)		0.00008	0.355	
PA6 (80 wt%) /PPS (20 wt%)	Chromium Steel	10 wt% Carbon Fibers (300 mesh)		0.00009	0.34	
PA6 (80 wt%) /PPS (20 wt%)	Chromium Steel	15 wt% Carbon Fibers (300 mesh)		0.0001	0.36	
PA66	PA66	x	Pin-on-Disk, 2 N, 0.2 m/s	0.00016	0.6	24
Nylon 6	Nylon 6	0	Block(Tab)-on-Disk, 5 N, 50 cm/s	0.0003	0.185	This study
Nylon 6	Nylon 6	5 vol% Ti <sub>3</sub> SiC <sub>2</sub>		0.0002	0.25	
Nylon 6	Nylon 6	10 vol% Ti <sub>3</sub> SiC <sub>2</sub>		0.00015	0.26	
Nylon 6	Nylon 6	15 vol% Ti <sub>3</sub> SiC <sub>2</sub>		0.00017	0.27	
Nylon 6	Nylon 6	20 vol% Ti <sub>3</sub> SiC <sub>2</sub>		0.00017	0.28	

Comparatively, during self-mating, the WR of UHMWPE surfaces was  $\sim 1.6 \times 10^{-4} \text{ mm}^3/\text{N.m}$ , whereas in 5 vol%  $\text{Ti}_3\text{SiC}_2$ -UHMWPE and 20 vol%  $\text{Ti}_3\text{SiC}_2$ -UHMWPE, the WR became negligible ( $< 4 \times 10^{-7} \text{ mm}^3/\text{N.m}$ ), thereafter, the total WR increased to  $\sim 2 \times 10^{-6} \text{ mm}^3/\text{N.m}$  in 35 vol%  $\text{Ti}_3\text{SiC}_2$ -UHMWPE [22]. Similarly, during self-mating,  $\text{Ti}_3\text{SiC}_2$ -PEEK composites showed better tribological behavior than PEEK, for example, as the  $\text{Ti}_3\text{SiC}_2$  content in PEEK was increased from 0 to 35 vol%, the  $\mu_{\text{mean}}$  decreased from  $\sim 0.19$  to  $\sim 0.14$  in PEEK-10% $\text{Ti}_3\text{SiC}_2$ , thereafter, it increased to  $\sim 0.21$  in PEEK-20% $\text{Ti}_3\text{SiC}_2$  and PEEK-30% $\text{Ti}_3\text{SiC}_2$ , respectively. PEEK-5% $\text{Ti}_3\text{SiC}_2$  tribocouple showed the lowest wear rate, and was 27 times more wear resistant than PEEK tribocouples [23].

From application perspective, polymer-on-polymer tribocouples are especially promising as polymers are light-weight and not susceptible to galvanic corrosion, but there has been limited studies on these tribocouples due to adhesive wear, lower thermal conductivity, among others [24]. Some of the applications of polymer-on-polymer devices are microbearings [25], and biomedical applications for cervical total disc replacement and joint replacements [26-28]. The aim of this Chapter III of current thesis is to synthesis of Nylon- $\text{Ti}_3\text{SiC}_2$  and Teflon- $\text{Ti}_3\text{SiC}_2$  composites and characterization of their tribological behavior during self-mating. In general, the composites of MAX phases and polymers are referred to as MAXPOLs [22, 23]. It is important to distinguish different types of MAXPOLs composites. In this Chapter III,  $< 30 \text{ vol}\%$   $\text{Ti}_3\text{SiC}_2$  is being used to fill the polymer matrix; thus, these types of novel composites will be referred to as MAX Reinforced Polymers (MRPs) to distinguish these novel composites from interpenetrating composites, or any other engineered derivatives.

### 3.2 Experimental Methods

Teflon (Polytetrafluoroethylene (PTFE), average particle size 20  $\mu\text{m}$ , Goodfellow Cambridge Limited, Huntingdon, England), Nylon (Nylon 6 (PA 6), average particle size 15-20  $\mu\text{m}$ , Goodfellow Cambridge Limited, Huntingdon, England) and  $\text{Ti}_3\text{SiC}_2$  (-325 mesh, 40-50  $\mu\text{m}$ , Kanthal, Hallstahammar, Sweden) powders were used to fabricate the composites. During this study four different compositions were designed by reinforcing PTFE matrix with 5 vol% (Teflon-5% $\text{Ti}_3\text{SiC}_2$ ), 10 vol% (Teflon-10% $\text{Ti}_3\text{SiC}_2$ ), 20 vol% (Teflon-20% $\text{Ti}_3\text{SiC}_2$ ), and 30 vol%  $\text{Ti}_3\text{SiC}_2$  (Teflon-30% $\text{Ti}_3\text{SiC}_2$ ), and Nylon matrix with 5 vol% (Nylon-5% $\text{Ti}_3\text{SiC}_2$ ), 10 vol% (Nylon-10% $\text{Ti}_3\text{SiC}_2$ ), 20 vol% (Nylon-20% $\text{Ti}_3\text{SiC}_2$ ), and 30 vol%  $\text{Ti}_3\text{SiC}_2$  (Nylon-30% $\text{Ti}_3\text{SiC}_2$ ), respectively. All the samples were produced by hot pressing (HP).

The required amount of powders were dry ball milled (8000 M mixer Mill, SPEX SamplePrep, Metuchen, NJ) for 30 minutes. All the powders were then poured in a die (EQ-Die-12D, MTI Corporation, Richmond, CA). The compositions were then sintered by hot pressing (HP) (Model EQ-HP-6T, MTI Corporation, Richmond, CA) in atmospheric air. During HP, samples were heated at 5° C/min to 350° C, then they were held at 350° C for 20 min, thereafter a uniaxial compressive stress of ~120 MPa was applied for 5 minutes, and the furnace was slowly cooled to ambient temperature. The hot pressed samples were then demolded from the die, and used for further characterization. For comparison, pristine Teflon and Nylon compacts were also prepared by following the above mentioned procedure.

Samples were mounted on aluminum mounts and coated with Au/Pd using a Balzers SCD 030 sputter coater (BAL-TEC RMC, Tucson, AZ). SE (Secondary Electron) and BSE (Back Scattered Electron) images were obtained by using a JEOL JSM-6490LV Scanning Electron Microscope

(JEOL USA, Inc., Peabody, Massachusetts). The hardness measurements were performed on polished samples by using a Shore D hardness indenter (Model OS-1E, Precision Durometer, Electromatic Equipment Co., Inc., Cedarhurst, NY). Porosity of the sample was calculated by normalizing the measured density with theoretical density of the composites. All the tribology studies were then performed by a block-on-disc tribometer (CSM Instruments SA, Peseux, Switzerland) at 5 N (~0.3 MPa), 50 cm/s linear speed, 5000 m sliding distance, and ~10 mm track radius. The HP samples were cut into tabs with dimensions of ~4 mm x ~4 mm (cross-section) x ~3 mm (thickness). The HP samples were also used as disks (substrates). For each composition, a set of three experiments were performed. A surface profilometer (Surfcom 480A, Tokyo Seimitsu Co. Ltd., Japan) was used to measure surface finish of all the samples after polishing. All the samples had  $R_a < 1 \mu\text{m}$  (arithmetic mean roughness). The data analysis was performed by calculating an average of friction coefficient readings during a single experiment; thereafter, an average of three mean values from three experiments was calculated and reported in the text as  $\mu_{\text{mean}}$ . The mass of the tabs and disks were measured before and after the testing by a weighing scale (XA 83/220/2X, Radwag, Radom, Poland). The specific wear rate (WR) was calculated from:

$$\text{WR} = (m_i - m_f) / (\rho N d) \text{ -----(I)}$$

where,  $m_i$  is the initial mass,  $m_f$  is the final mass,  $\rho$  is density of the composite,  $N$  is the applied load, and  $d$  is the total distance traversed by the static during the tribology testing. In the text, total WR of both the tabs and disks is reported and will be referred to as WR [21-23].

### 3.3 Results and Discussion

#### 3.3.1 Investigation of the Microstructures

Figure 3.1 shows the SEM micrographs of  $\text{Ti}_3\text{SiC}_2$ -Teflon composites. In general,  $\text{Ti}_3\text{SiC}_2$  particulates are well-dispersed in the Teflon matrix. Figure 3.2 shows the SEM micrographs of

Ti<sub>3</sub>SiC<sub>2</sub>-Nylon composites. Ti<sub>3</sub>SiC<sub>2</sub> particulates are well-dispersed in the Nylon matrix at lower concentration (<10 vol%), but at higher concentrations, these particles are dispersed at phase boundaries of the composites (Fig. 3.2f). Similar behavior was also observed in Ti<sub>3</sub>SiC<sub>2</sub>-UHMWPE composites where Ti<sub>3</sub>SiC<sub>2</sub> segregated to the phase boundaries due to dewetting [22]. Figure 3.3 plots the variation of porosity (Y1 axis) and hardness (Y2 axis) versus Ti<sub>3</sub>SiC<sub>2</sub> concentration.

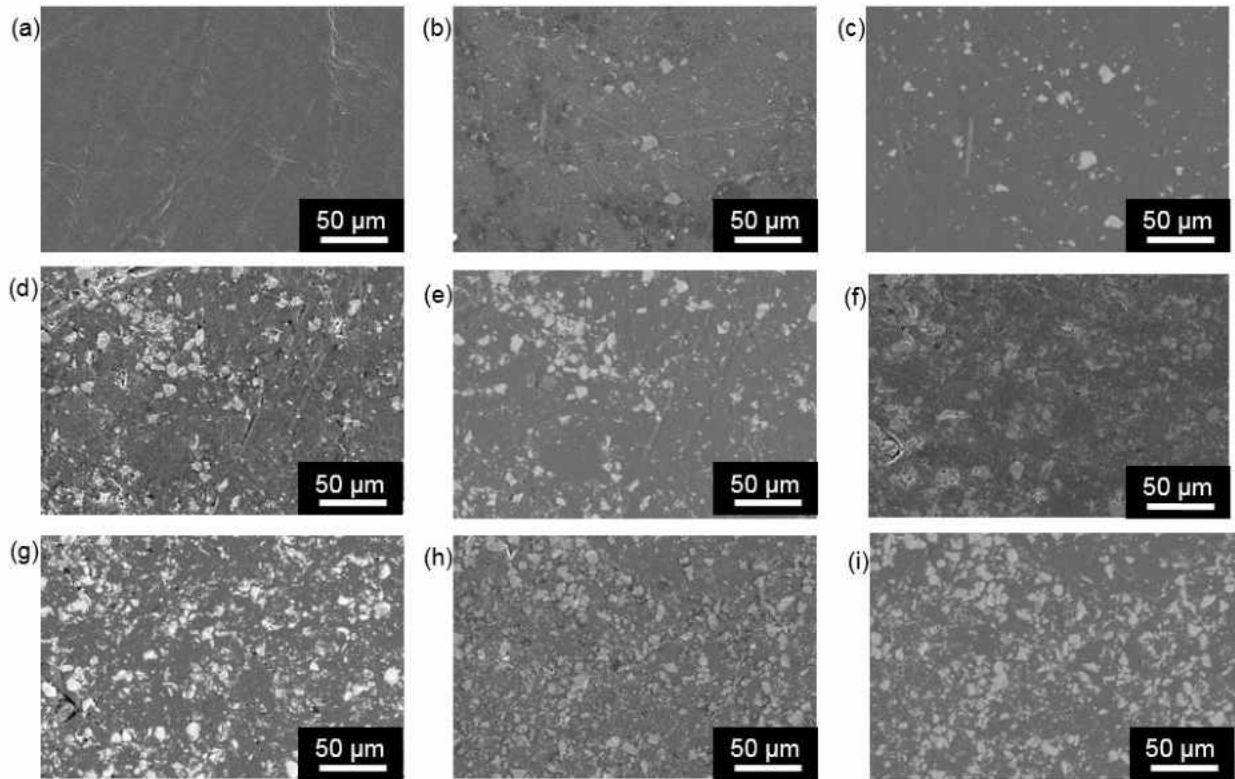


Figure 3.1 SE SEM micrographs (a) Teflon, (b) Teflon-5%Ti<sub>3</sub>SiC<sub>2</sub>, (c) BSE image of the same region, (d) Teflon-10%Ti<sub>3</sub>SiC<sub>2</sub>, (e) BSE image of the same region, (f) Teflon-20%Ti<sub>3</sub>SiC<sub>2</sub>, (g) BSE image of the same region, (h) Teflon-30%Ti<sub>3</sub>SiC<sub>2</sub>, and (i) BSE image of the same region.

In general, the porosity of the samples increased as the concentration of Ti<sub>3</sub>SiC<sub>2</sub> was increased in the particulate matrix which further corroborates the presence of porosities during SEM analysis

(Figs. 3.1 and 3.2). Previous studies on composites composed of  $Ti_3SiC_2$ -UHMWPE, and  $Ti_3SiC_2$ -PEEK had also yielded similar results [22, 23].

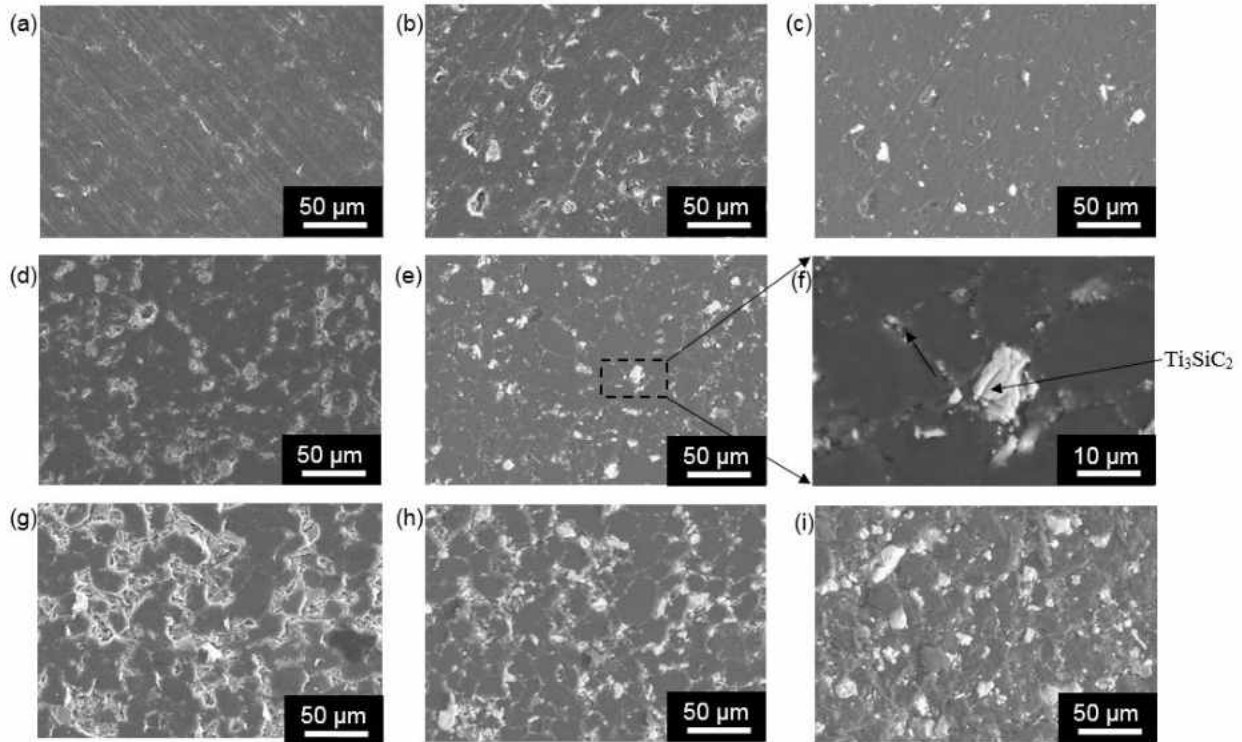


Figure 3.2 SE SEM micrographs (a) Nylon, (b) Nylon-5% $Ti_3SiC_2$ , (c) BSE image of the same region, (d) Nylon-10% $Ti_3SiC_2$ , (e) BSE image of the same region, (f) higher magnification of the marked region, (g) Nylon-20% $Ti_3SiC_2$ , (h) BSE image of the same region, and (i) BSE image of Nylon-30% $Ti_3SiC_2$ .

Briefly, the addition of  $Ti_3SiC_2$  particulates increases the stiffness of the compacted samples during processing which hinders the densification of these composites. As a result, the hardness of the samples increased as the concentration of  $Ti_3SiC_2$  particulates was increased in the polymer matrix (Fig. 3.3).

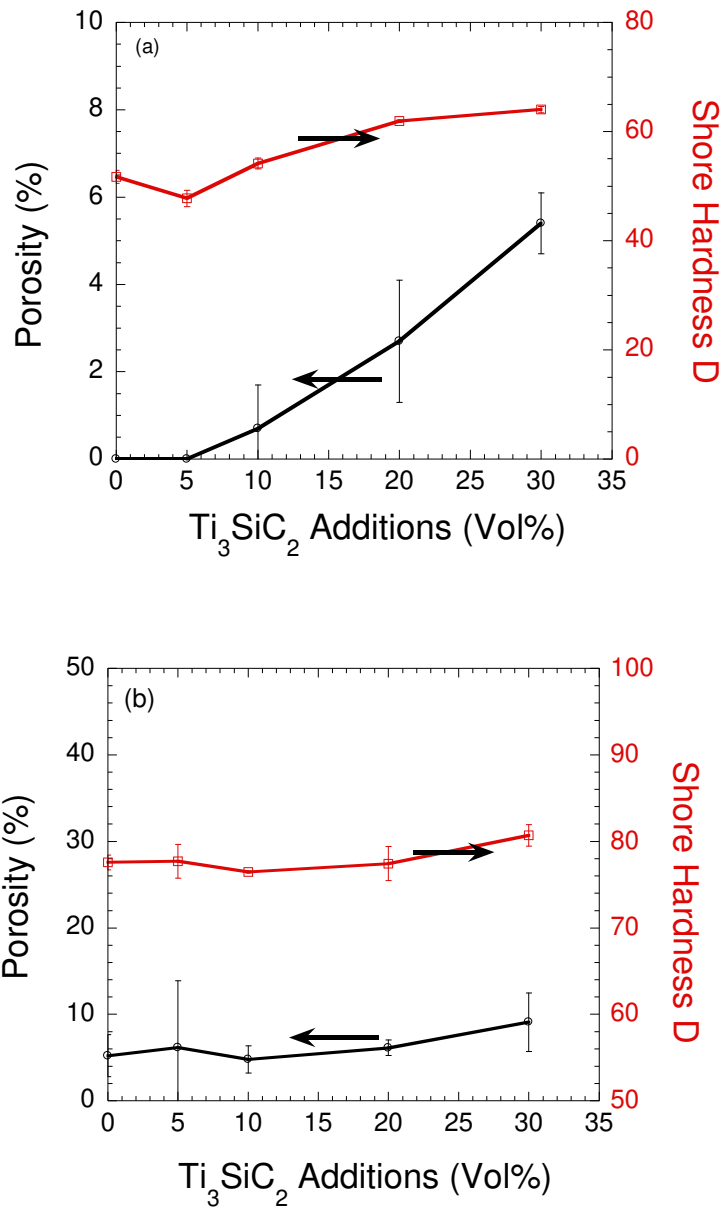


Figure 3.3 Plot of Porosity (Y1 axis) and Hardness (Y2 axis) versus  $Ti_3SiC_2$  additions for (a) Teflon- $Ti_3SiC_2$ , and (b) Nylon- $Ti_3SiC_2$  composites.

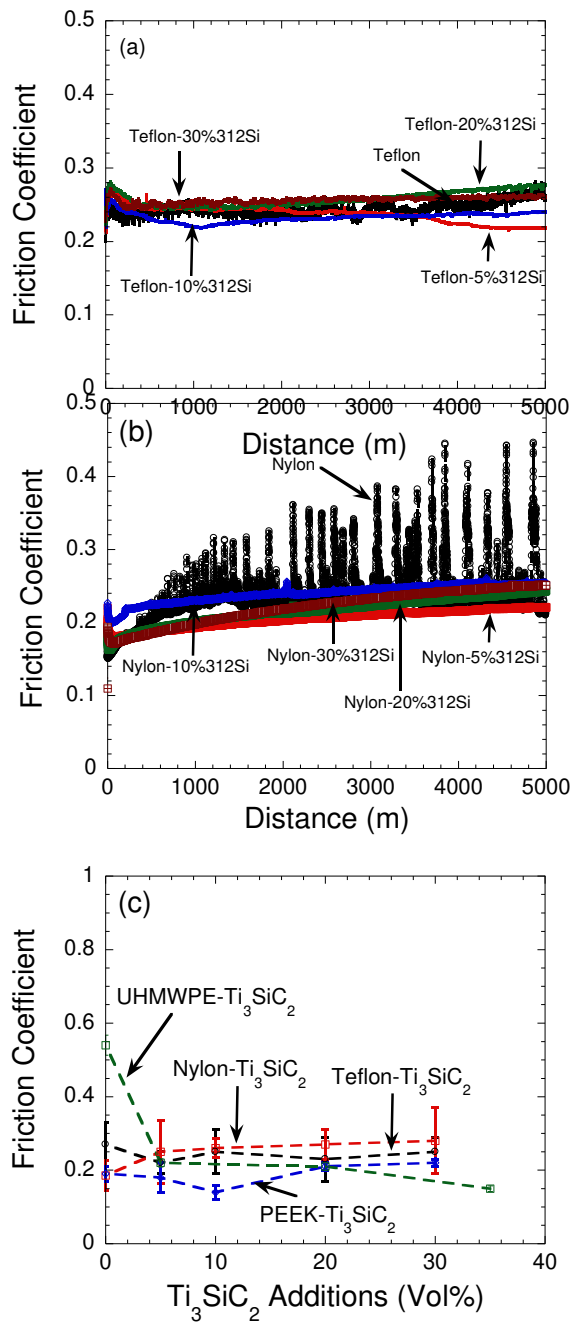


Figure 3.4 Plot of friction coefficient versus ( $\mu$ ) sliding distance of different compositions of (a)  $Ti_3SiC_2$ -Teflon, (b)  $Ti_3SiC_2$ -Nylon, and (c) mean friction coefficient ( $\mu_m$ ) versus  $Ti_3SiC_2$  additions (vol%) (data of  $Ti_3SiC_2$ -UHMWPE [22] and  $Ti_3SiC_2$ -PEEK [23] composites are also inserted in the plot to show comparison).

### 3.3.2 Tribological Behavior

Figures 3.4a and 3.4b show  $\mu$  versus distance profiles of different  $\text{Ti}_3\text{SiC}_2$ -Teflon and  $\text{Ti}_3\text{SiC}_2$ -Nylon composites during self-mating, respectively. In the former case (Fig. 3.4a),  $\mu$  was stable during the tribological testing for all compositions, whereas  $\text{Ti}_3\text{SiC}_2$ -Nylon composites during self-mating showed stable  $\mu$  as a function of distance as compared to Nylon which showed erratic behavior. More particularly,  $\mu_{\text{mean}}$  decreased marginally from  $\sim 0.27$  in Teflon to  $\sim 0.25$  in Teflon-30%312Si, whereas  $\mu_{\text{mean}}$  increased gradually from  $\sim 0.185$  in Nylon to  $\sim 0.28$  in Nylon-30%312Si, respectively (Fig. 3.4c). Comparatively, the overall trend in  $\mu_{\text{mean}}$  was very similar to  $\text{Ti}_3\text{SiC}_2$ -PEEK whereas  $\text{Ti}_3\text{SiC}_2$ -UHMWPE composites showed a more pronounced effect (Fig. 3.4a) [22, 23]. The potential mechanism will be discussed in the next section.

The WR of Teflon was  $(7\pm 1) \times 10^{-4} \text{ mm}^3/\text{N.m}$  (Fig. 3.5a), it decreased to  $(5\pm 3) \times 10^{-5} \text{ mm}^3/\text{N.m}$  and  $(1\pm 1.5) \times 10^{-5} \text{ mm}^3/\text{N.m}$  in Teflon-5%312Si and Teflon-10%312Si, respectively, and thereafter retained a similar value of  $(1.6\pm 1.6) \times 10^{-5}$  in Teflon-30%312Si samples. The WR of Nylon decreased marginally from  $(3\pm 2) \times 10^{-4} \text{ mm}^3/\text{N.m}$  in Nylon to  $(1.7\pm 1.2) \times 10^{-4}$  in Nylon-30%312Si samples (Fig. 3.5a).  $\text{Ti}_3\text{SiC}_2$ -PEEK samples showed similar trend whereas in  $\text{Ti}_3\text{SiC}_2$ -UHMWPE composites, the WR almost became negligible in UHMWPE-5%312Si and UHMWPE-20%312Si compositions ( $\text{WR} < 4 \times 10^{-7} \text{ mm}^3/\text{N.m}$ ) (Fig. 3.5a).

It is very difficult to compare tribological results of different groups as these are done under different conditions which are dependent on various applications. In general, the WR of Teflon during self-mating [24], and against different substrates varied between  $10^{-3}$ - $10^{-4} \text{ mm}^3/\text{N.m}$  which are in the similar range as our results.

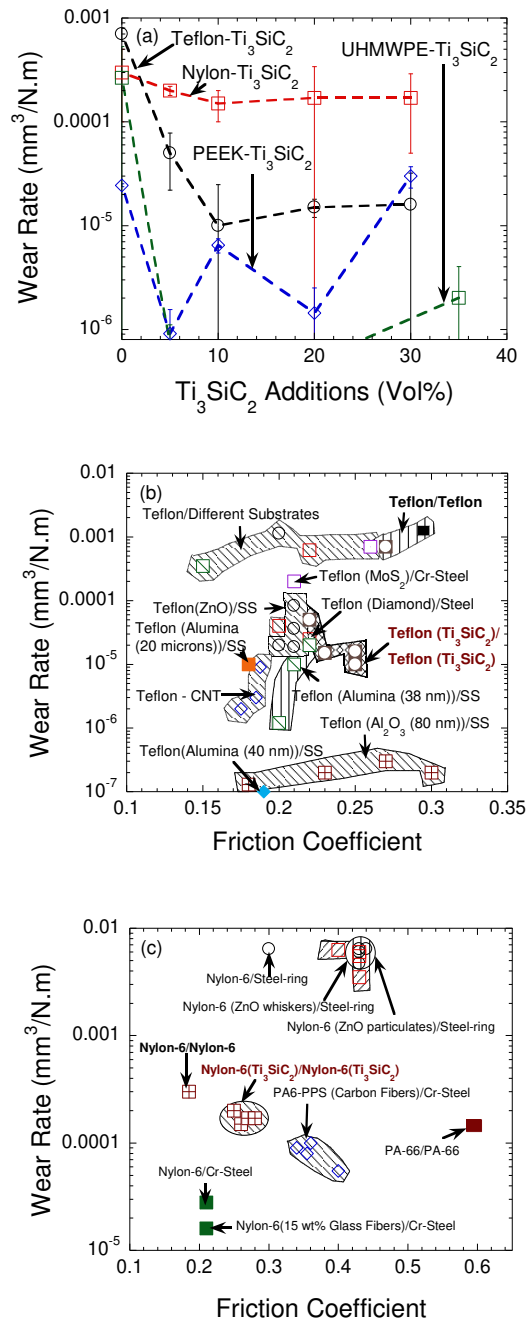


Figure 3.5 Plot of (a) WR versus Ti<sub>3</sub>SiC<sub>2</sub> additions (data of UHMWPE-Ti<sub>3</sub>SiC<sub>2</sub> and PEEK-Ti<sub>3</sub>SiC<sub>2</sub> is inserted for comparison [22-23]), and WR versus friction coefficient of different, (b) Teflon-based composites [Table 3.1], and (c) Nylon-based composites against different substrates

For qualitative comparison, Figure 3.5b summarizes the WR versus  $\mu$  plot of different Teflon-based composite systems (for detailed references – please see Table 3.1). The self-lubricating and self-mating  $\text{Ti}_3\text{SiC}_2$ -Teflon tribocouples compares favorably with composites fabricated by the additions of ZnO [2], ultrafine diamond [3],  $\text{MoS}_2$  [4],  $\text{B}_2\text{O}_3$  [5], and  $\text{Al}_2\text{O}_3$  (micron sized particulates) [8]. These results are especially significant as they were observed during self-mating which open new avenues of novel polymer-on-polymer composites. Polymer based nanocomposites showed better results than the self-mating  $\text{Ti}_3\text{SiC}_2$ -Teflon composites. McElwain et al. [8] showed that the Teflon matrix filled with nano-fillers of alumina performed better than micron-sized fillers as nanocomposites deposited a thinner, well-adhered transfer film that is stable and consequently not abraded by nano-fillers (Fig. 3.5b, Table 3.1). Burriss and Sawyer [9] in their pioneering work showed that irregular sized nano-fillers of alumina performed better than spherical nano-fillers of alumina. Later, Ye et al. [10] proposed that the tribology of these nanocomposites are governed by a complex interplay of transfer film adhesion, chemistry, debris morphology, and mechanics. For future studies, the effect of nano-fillers of  $\text{Ti}_3\text{SiC}_2$  on the tribological behavior of Teflon-based composites will give a more direct comparison with nano-composites.

Figure 3.5c summarizes WR versus  $\mu$  plot of different Nylon-based composite systems. The detailed data and references are listed in Table 3.2. Self-mating tribocouples of  $\text{Ti}_3\text{SiC}_2$ -Nylon composites compare favorably with ZnO (particulates or whiskers) [11], and other fibrous fillers [12, 14]. There have been very few studies to study the self-mating of Nylon-nylon tribocouples [24, 29]. For example, Jia et al. [24] observed higher wear in Nylon-Nylon self-mating by using oil lubrication as compared to dry lubrication due to reduction in mechanical strength because of the diffusion of oil into the outer layer. The prospect of using  $\text{Ti}_3\text{SiC}_2$  particulates as antiwear

additive offers materials scientist more options for designing Nylon based polymer-on-polymer devices.

### 3.3.3 Investigation of Tribosurfaces and Potential Mechanisms

Figure 3.6 shows the SEM micrographs of the Teflon (Figs.3.6a-b) and Teflon-20% $\text{Ti}_3\text{SiC}_2$  (Figs. 3.6c-f) tribocouples after the tribology testing. The Teflon surface (Figs. 3.6a-b) is riddled with adhesive wear marks. Comparatively, Teflon-20% $\text{Ti}_3\text{SiC}_2$  samples (Figs. 3.6c-f) showed minimal damage due to adhesive wear and minimal mass transfer between the tribosurfaces. In other words, no tribofilms was observed on both tribo-surfaces. The  $\text{Ti}_3\text{SiC}_2$  particulates showed signs of mild oxidation (Fig. 3.6d). Comparably, Fig. 3.7 shows the SEM micrographs of Nylon (Figs.3.7a-b) and Nylon-20% $\text{Ti}_3\text{SiC}_2$  (Figs. 3.7c-f) tribocouples after the tribology testing. Nylon surfaces showed signs of adhesive wear whereas both surfaces of Nylon-20% $\text{Ti}_3\text{SiC}_2$  showed features like polymer ligaments, pull-out of  $\text{Ti}_3\text{SiC}_2$  particulates due to abrasive wear by  $\text{Ti}_3\text{SiC}_2$  particulates. In addition,  $\text{Ti}_3\text{SiC}_2$  particulates did not show any oxidation which indicates that there is no transfer film at the interface (Inset of Fig. 3.7f). By analyzing the two composite systems, it is clear that interactions between polymer and  $\text{Ti}_3\text{SiC}_2$  particulates play a very critical role in wear determining process. Figure 3.8 shows simple schematics to summarize the tribological process. Adhesive wear is observed during self-mating of Teflon and Nylon (Figs. 3.8a1-a2). It is widely accepted in literature that the wear between polymer tribocouples is due to adhesion, and the exact mechanism has been a subject of detailed fundamental studies [24, 30, 31]. Based on the recent data [22], the tribological behavior of the MRPs during self-mating can be divided into three different scenarios. During case A, for example,  $\text{Ti}_3\text{SiC}_2$ -UHMWPE composites [22], if the

$Ti_3SiC_2$  particulates remain embedded in the polymer matrix during the tribological process then mild adhesive wear is accompanied by the formation of type IIIa tribofilms (Figs. 3.8b1-b2).

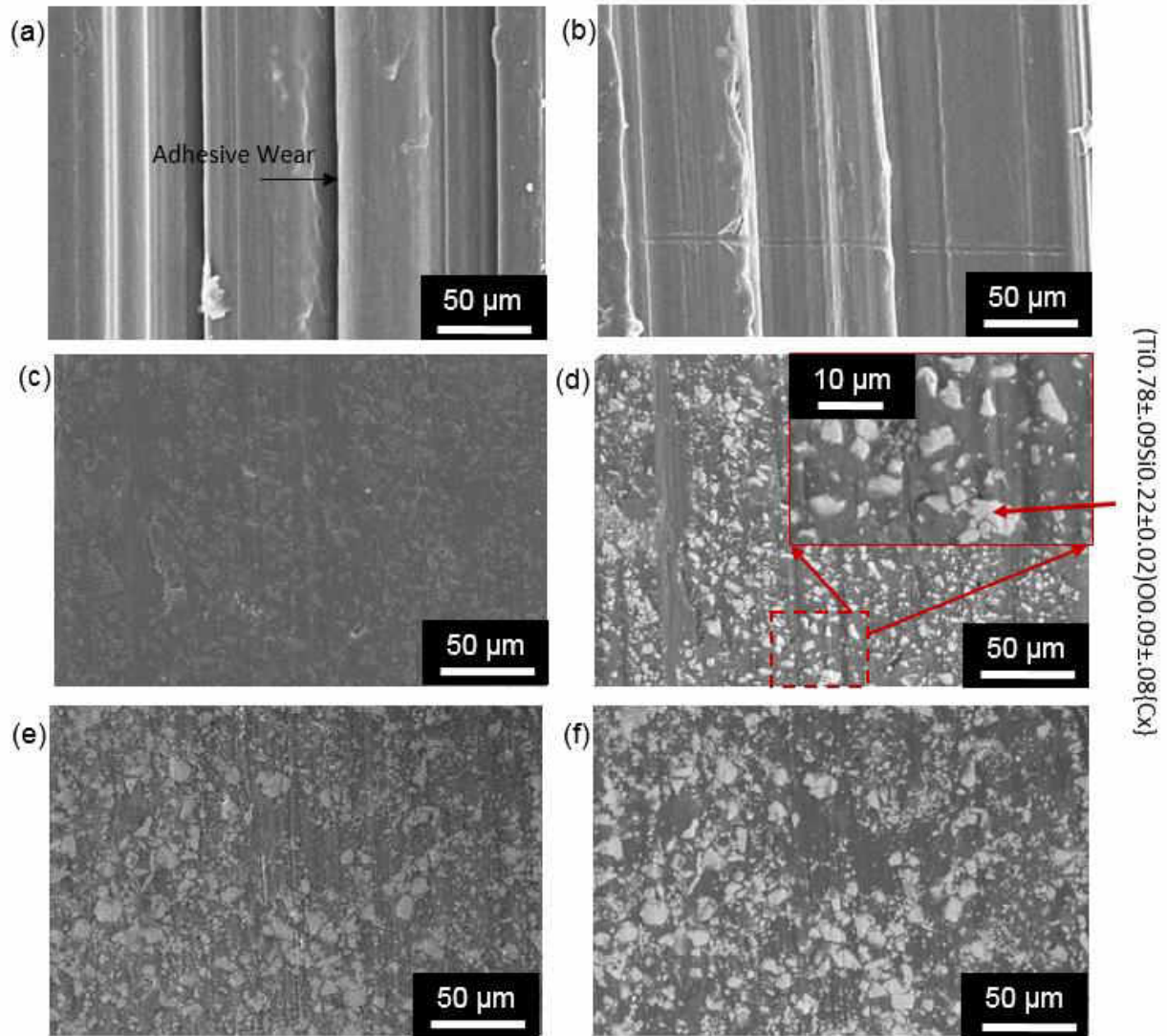


Figure 3.6 SE SEM micrographs of (a) Teflon (block), (b) Teflon (disk), (c) Teflon-20%312Si (block), (d) BSE image of the same region (inset shows the higher magnification of the region marked in (d)), (e) Teflon-20%312Si (disk), and (f) BSE image of the same region after tribological testing.

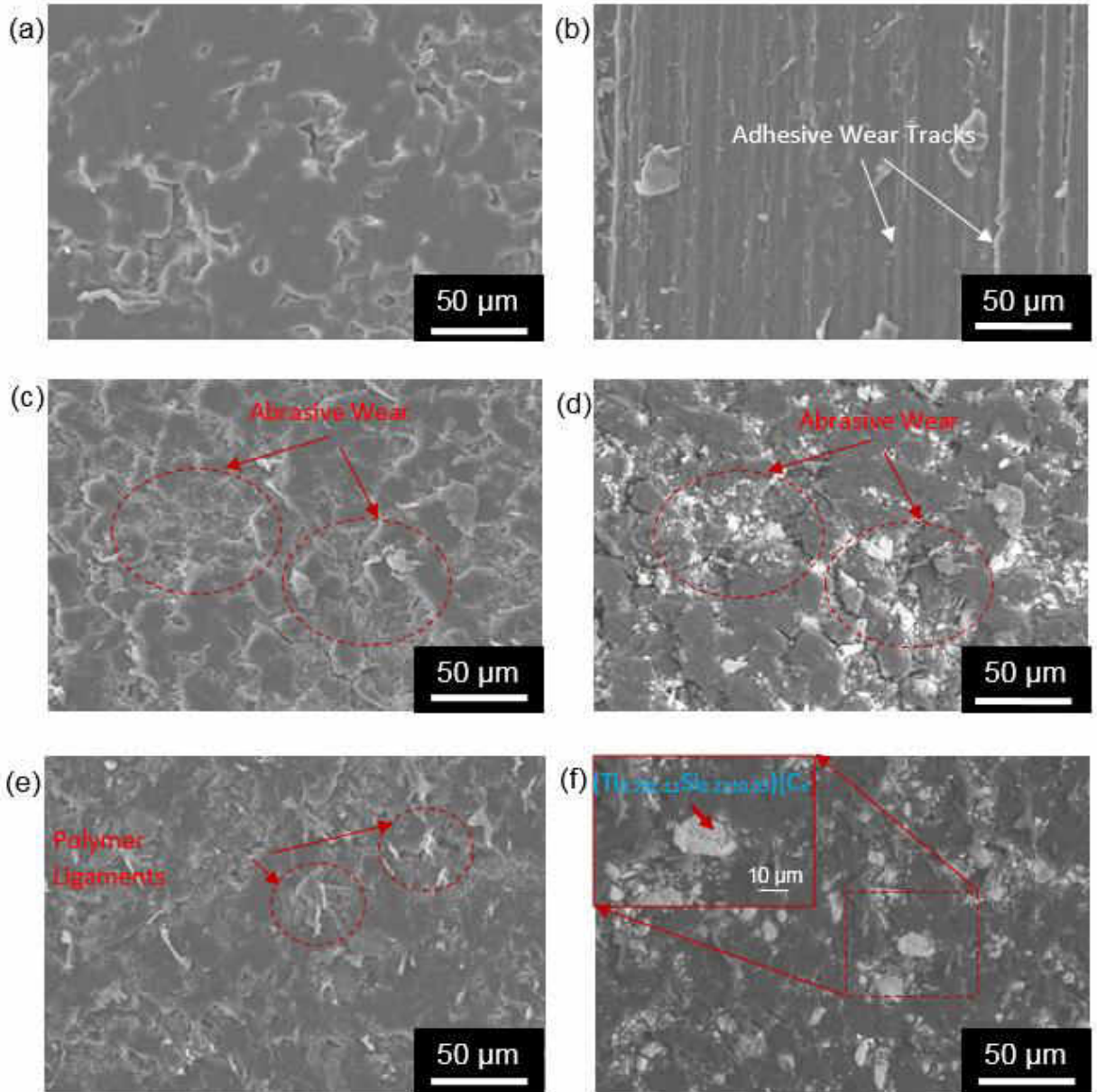


Figure 3.7 SE SEM micrographs of (a) Nylon (block), (b) Nylon (disk), (c) Nylon-20%312Si (block), (d) BSE image of the same region, (e) Teflon-20%312Si (disk), and (f) BSE image of the same region after tribological testing (inset shows the higher magnification of the region marked in (f)).

As a background, Gupta and Barsoum [19] had proposed a classification system for tribofilms according to triboreactions. Type III tribofilms are formed by triboreactions at both the counter and MAX or MAX based composite surfaces. These tribofilms were further classified into different sub-categories by taking into account the architecture of the tribofilms and chemical reactions. Type IIIa tribofilms were classified as those tribofilms which are barely visible to naked eyes and for amorphous thin layers over each tribosurface by SEM analysis. During Case B, mild adhesive wear tracks and no visible tribofilms were observed [Fig. 8c1-c2]. There were no signs of abrasive wear in the polymer matrix which indicates that  $Ti_3SiC_2$  particles are well adherent in the polymer matrix. This type of behavior was observed in  $Ti_3SiC_2$ -PEEK [23] and  $Ti_3SiC_2$ -Teflon composites. The WR is however high as compared to Case A (Fig. 3.5a) which further indicate as tribofilms are not able to adhere to tribosurfaces or too thin to be observed by SEM analysis thus the WR is higher as compared to case A, but the presence of  $Ti_3SiC_2$  particulates are able to reduce the adhesive wear at dry contacts which accounts for better tribological performance than the respective pristine polymer-polymer tribocouples. In other words, the formation of adherent tribofilms lowers the WR by protecting the substrates in Case A as compared to the latter case where no tribofilms are observed. In general, tribofilms are observed during tribology of polymer matrix composites filled with inorganic particles [32-34]. Bahadur [34] had also summarized that the effectiveness of tribofilms to protect the substrates will depend on, (a) the cohesion of transfer film, (b) adhesion between transfer film and counterface, and (c) the protection of rubbing polymer surface from metal asperities by transfer film.

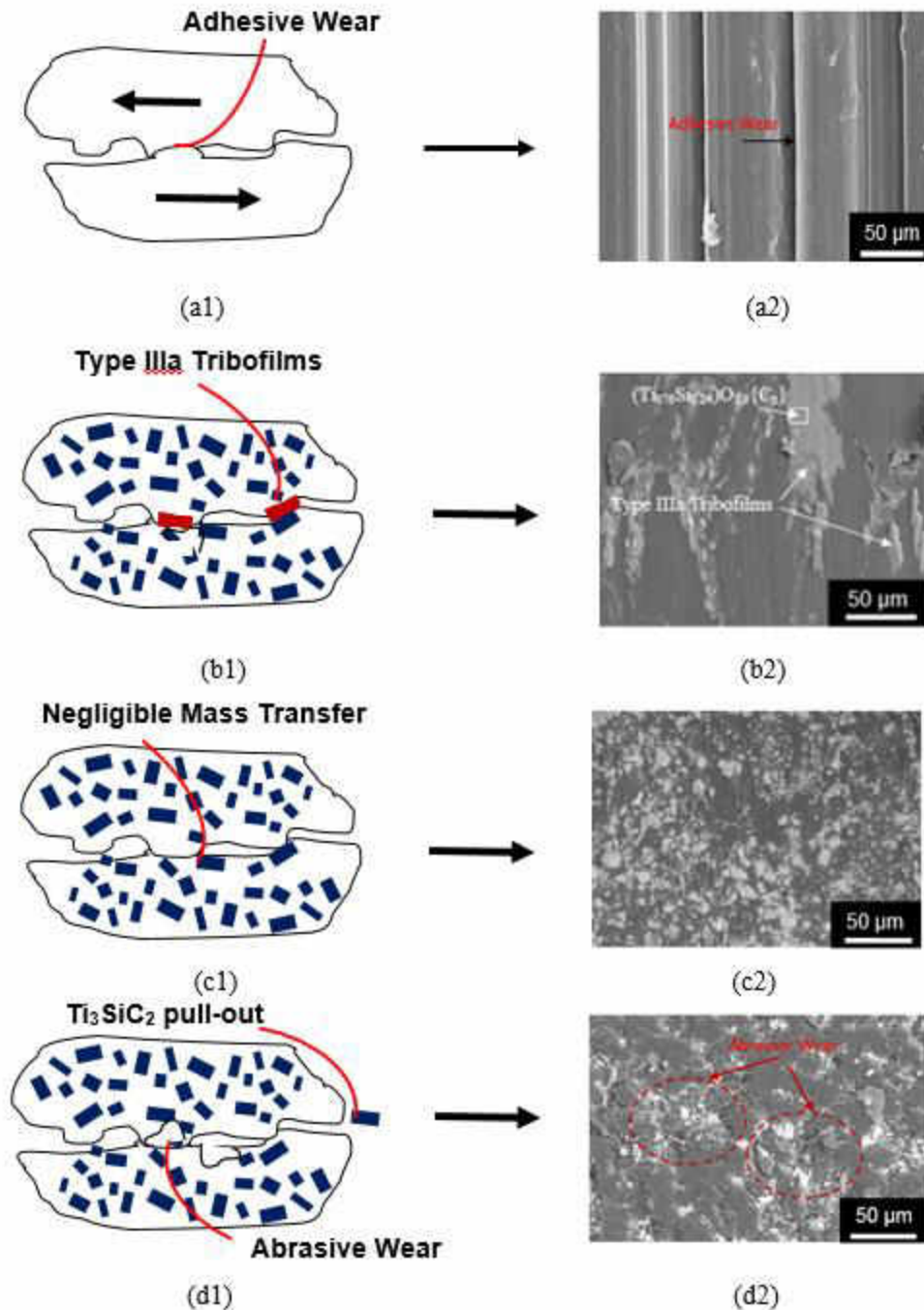


Figure 3.8 Schematics of (a1) adhesive wear in polymer-polymer composites, (a2) SEM micrograph showing adhesive wear (Fig. 3.6), (b1) Type IIIa tribofilms, (b2) SEM micrograph showing Type IIIa tribofilm [22], (c1) Negligible mass transfer between tribocouples, (c2) SEM micrograph of Teflon-20%312Si surface (Fig. 3.6), (d1) Abrasive wear at tribocontacts due to the pull out of  $Ti_3SiC_2$  particulates, and (d2) SEM micrograph showing abrasive wear (Fig. 3.7).

During Case C, for example  $\text{Ti}_3\text{SiC}_2$ -Nylon composites, the excessive debonding of  $\text{Ti}_3\text{SiC}_2$  particles during tribological process caused abrasive wear, and resulted in higher WR as compared to both Cases A and B (Fig. 3.8d1-d2). It is important to note that in spite of the abrasive wear observed in Nylon- $\text{Ti}_3\text{SiC}_2$  composites, the overall wear of these composites are slightly lower than the Nylon-Nylon tribocouples (Table 3.2). Based on current results, it can be surmised that  $\text{Ti}_3\text{SiC}_2$ -polymer composites during self-mating performs comparably to different polymer-metal tribocouples, and are promising materials for different tribological applications. It is further hypothesized that the properties of MRPs can be further enhanced by increasing bonding between the polymer and  $\text{Ti}_3\text{SiC}_2$  particulates and decreasing the size of  $\text{Ti}_3\text{SiC}_2$  particulates.

### 3.4 Conclusions

$\text{Ti}_3\text{SiC}_2$ -Teflon and  $\text{Ti}_3\text{SiC}_2$ -Nylon composites were synthesized for the first time. SEM evaluation showed that  $\text{Ti}_3\text{SiC}_2$  particulates are well dispersed in the Teflon matrix, whereas  $\text{Ti}_3\text{SiC}_2$  particulates showed dewetting and they were present in the phase boundaries in Nylon matrix. During self-mating,  $\text{Ti}_3\text{SiC}_2$ -Teflon composites showed better performance than  $\text{Ti}_3\text{SiC}_2$ -Nylon composites. For example,  $\mu_{\text{mean}}$  decreased marginally from  $\sim 0.27$  in Teflon to  $\sim 0.25$  in Teflon-30% $\text{Ti}_3\text{SiC}_2$  and the concomitant WR of Teflon was  $(7 \pm 1) \times 10^{-4} \text{ mm}^3/\text{N.m}$  and it decreased to  $(5 \pm 3) \times 10^{-5} \text{ mm}^3/\text{N.m}$  and  $(1 \pm 1.5) \times 10^{-5} \text{ mm}^3/\text{N.m}$  in Teflon-5% $\text{Ti}_3\text{SiC}_2$  and Teflon-10% $\text{Ti}_3\text{SiC}_2$ , respectively, and thereafter retained a similar value of  $(1.6 \pm 1.6) \times 10^{-5}$  in Teflon-30% $\text{Ti}_3\text{SiC}_2$ . Comparatively,  $\mu_{\text{mean}}$  increased gradually from  $\sim 0.185$  in Nylon to  $\sim 0.28$  in Nylon-30% $\text{Ti}_3\text{SiC}_2$ , and the concomitant WR of Nylon decreased marginally from  $(3 \pm 2) \times 10^{-4} \text{ mm}^3/\text{N.m}$  in Nylon to  $(1.7 \pm 1.2) \times 10^{-4}$  in Nylon-30% $\text{Ti}_3\text{SiC}_2$  samples. After evaluating the tribosurfaces by SEM analysis, three different scenarios were identified for understanding the tribological performance of MRPs.

## CHAPTER IV

### CONCLUSION AND SCOPE OF FUTURE STUDIES

#### 4.1 Conclusion

PEEK-Ti<sub>3</sub>SiC<sub>2</sub>, Teflon-Ti<sub>3</sub>SiC<sub>2</sub>, and Nylon-Ti<sub>3</sub>SiC<sub>2</sub> composites were synthesized and characterized for the first time. In these three set of MRPs, it was observed that the porosity of the samples increased as a function of Ti<sub>3</sub>SiC<sub>2</sub> content in the polymer matrix. More particularly, in Teflon-Ti<sub>3</sub>SiC<sub>2</sub> and Nylon-Ti<sub>3</sub>SiC<sub>2</sub> composites, the hardness of the samples increased as a function of Ti<sub>3</sub>SiC<sub>2</sub> content, whereas in PEEK-Ti<sub>3</sub>SiC<sub>2</sub> composites, an increase in hardness was observed until 5 vol% of Ti<sub>3</sub>SiC<sub>2</sub> addition, thereafter the hardness decreased with the further addition of Ti<sub>3</sub>SiC<sub>2</sub>.

During self-mating, PEEK-Ti<sub>3</sub>SiC<sub>2</sub> composites showed better performance than the Teflon-Ti<sub>3</sub>SiC<sub>2</sub> and Nylon-Ti<sub>3</sub>SiC<sub>2</sub> composites. For example, the friction coefficient of the PEEK-Ti<sub>3</sub>SiC<sub>2</sub> composites decreased from 0.19 to 0.14 when 10 vol% of Ti<sub>3</sub>SiC<sub>2</sub> was added; whereas in Teflon-Ti<sub>3</sub>SiC<sub>2</sub> the friction coefficient decreased from 0.27 to 0.25 when Ti<sub>3</sub>SiC<sub>2</sub> content was increased to 30 vol%, and in Nylon-Ti<sub>3</sub>SiC<sub>2</sub> composites, the friction coefficient increased from 0.185 to 0.28 as 30 vol% of Ti<sub>3</sub>SiC<sub>2</sub> was added in the Nylon matrix. Also, PEEK-Ti<sub>3</sub>SiC<sub>2</sub> composites showed better wear resistance than the Teflon-Ti<sub>3</sub>SiC<sub>2</sub> and Nylon-Ti<sub>3</sub>SiC<sub>2</sub> composites. The PEEK-5%Ti<sub>3</sub>SiC<sub>2</sub> showed 27 times more wear resistance than the pure PEEK. In Teflon-Ti<sub>3</sub>SiC<sub>2</sub> composites, the wear rate decreased from  $(7 \pm 1) \times 10^{-4} \text{ mm}^3/\text{N.m}$  to  $(1 \pm 1.5) \times 10^{-5} \text{ mm}^3/\text{N.m}$  when 10 vol% Ti<sub>3</sub>SiC<sub>2</sub> was added in the Teflon matrix, and in Nylon-Ti<sub>3</sub>SiC<sub>2</sub> composites, the wear rate

decreased marginally from  $(3\pm 2) \times 10^{-4} \text{ mm}^3/\text{N.m}$  in Nylon to  $(1.7\pm 1.2) \times 10^{-4}$  in Nylon-30% $\text{Ti}_3\text{SiC}_2$  samples.

In summary, all three set of composites exhibited better solid lubrication and tribological behavior than the pristine polymer, which show that  $\text{Ti}_3\text{SiC}_2$  can be used as an anti-wear additive to the polymer matrix. These results also open a new avenue for designing polymer-on-polymer tribocouples.

#### **4.2 Scope of Future Studies**

During all the studies,  $\text{Ti}_3\text{SiC}_2$  was the only MAX phase used to synthesize different MRPs although different polymers were used as matrices. It is further recommended that during the next phase of this research should focus on studying the effect of different M and A group on MRPs. All the samples were fabricated by using micron ( $\mu\text{m}$ ) sized particulates of MAX phases. By analyzing the Figures 3.5b and 3.5c, it can be concluded that nanosize (nm) particle performs better as filler materials than micron size particles for tribological study. In general, the friction coefficient and wear rate are lower for nanosize filler materials into polymer matrix as compared to micron size particles in the polymer matrix. It would be interesting to study the effect of nanosized MAX phase particles in the polymer matrix.

In this chapter, preliminary results on manufacturing of MRPs by using  $\text{Cr}_2\text{AlC}$ ,  $\text{Cr}_2\text{GaC}$ , and  $\text{V}_2\text{AlC}$  particulates in the PEEK matrix will be presented.

#### **4.3 Experimental Methods**

PEEK (average particle size  $20 \mu\text{m}$ , Goodfellow Cambridge Limited, Huntingdon, England) and  $\text{Cr}_2\text{AlC}$  or  $\text{Cr}_2\text{GaC}$  or  $\text{V}_2\text{AlC}$  (-325 mesh) powders were used to fabricate composites. During this study, four different compositions for each MAX phase were designed by reinforcing PEEK

matrix with 5 vol.% (PEEK–5% Cr<sub>2</sub>AlC or Cr<sub>2</sub>GaC or V<sub>2</sub>AlC), 10 vol.% (PEEK–10% Cr<sub>2</sub>AlC or Cr<sub>2</sub>GaC or V<sub>2</sub>AlC), 20 vol.% (PEEK–20% Cr<sub>2</sub>AlC or Cr<sub>2</sub>GaC or V<sub>2</sub>AlC), and 30 vol.% Ti<sub>3</sub>SiC<sub>2</sub> (PEEK–30% Cr<sub>2</sub>AlC or Cr<sub>2</sub>GaC or V<sub>2</sub>AlC), respectively. All the samples were produced by hot pressing (HP). The required amount of powders were dry ball milled (8000M mixer Mill, SPEX SamplePrep, Metuchen, NJ) for 30 min. All the powders were then poured in a die (EQ-Die-12D, MTI Corporation, Richmond, CA). The compositions were then sintered by HP (Model EQ-HP-6T, MTI Corporation, Richmond, CA) in atmospheric air. During HP, samples were heated at 5° C/min to 450° C, then they were held at 450° C for 20 min, thereafter a uniaxial compressive stress of ~120 MPa was applied for 5 min, and the furnace was slowly cooled to ambient temperature. The hot pressed samples were then demolded from the die, and used for further characterization. For comparison, pristine PEEK compacts were also prepared by following the above mentioned procedure. Prior to hardness testing all composites were polished (Ra<1 mm) and then tested on a Vicker's micro hardness indenter (Mitutoyo HM-112, Mitutoyo Corporation, Aurora, IL).

Vicker's hardness was measured by loading the samples at 2.9N for 15 s. An average of five readings for each composite was measured and is reported in this text. The rule of mixtures was used to calculate the theoretical density of the PEEK-MAX composites. The mass and dimensions of each sample were measured and the experimental density then calculated. Using the experimental and theoretical density, the relative density and porosity was calculated in this chapter.

#### 4.4 Results and discussion

Figure 4.1 shows the change in porosity as a function of MAX phases. In general, as the concentration of MAX phase particulates were increased in the PEEK matrix, the porosity in the sample increased. Figure 4.2 shows the change in hardness as a function of MAX phases content. In most of the cases, an increase in hardness was observed when 5 vol% MAX phase added to the PEEK matrix, thereafter hardness decreased as the concentration of MAX phase was increased.

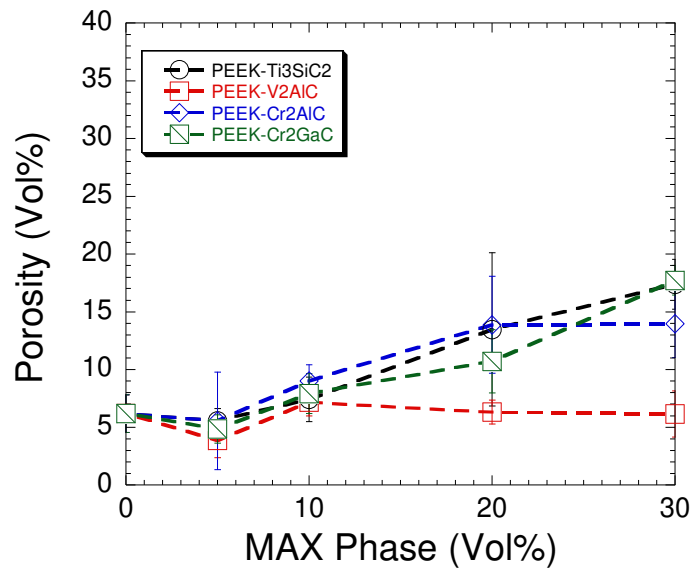


Figure 4.1 Plot of Porosity versus MAX phase content

However, in PEEK-Cr<sub>2</sub>AlC composites, an increased in hardness was observed until 10 vol% addition of MAX phase into the PEEK matrix, thereafter the hardness started to decrease. More studies are needed to understand the mechanical and tribological behavior of these composites.

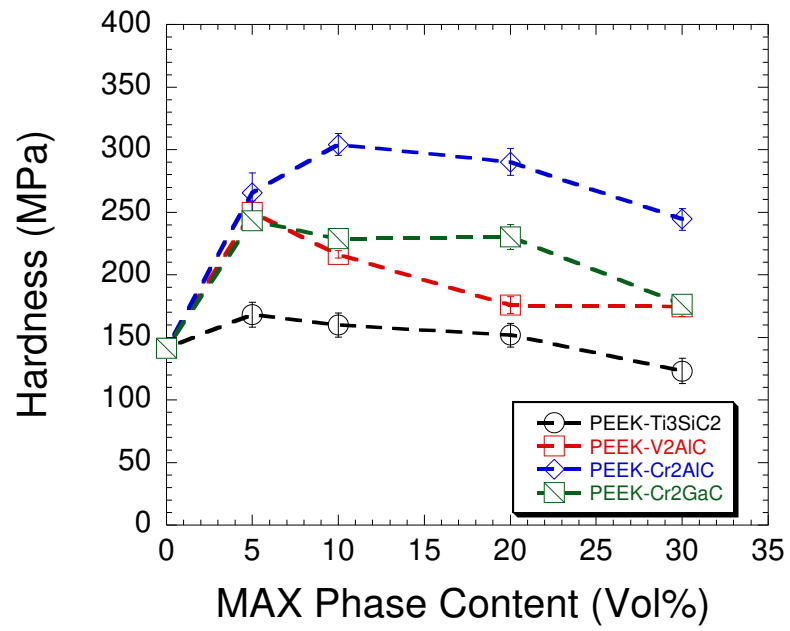


Figure 4.2 Plot of Hardness versus MAX phase content

## APPENDIX

### References

#### CHAPTER I

- [1] “The MAX Phases: Unique New Carbide and Nitride Materials”, M. W. Barsoum, Tamer-El-Raghy, *American Scientist*, Volume 89, P 334, (2001).
- [2] “On the tribology of the MAX phases and their composites during dry sliding: A review”, S. Gupta, M. W. Barsoum, *Wear*, Volume 271, P 1878– 1894 (2011).
- [3] “Encyclopedia of Materials Science and Technology”, M.W. Barsoum, M. Radovic, R. W. Chan, K.H.J. Buschow, M.C. Flemings, E.J. Kramer, S. Mahajan, P. Veysiere (Eds.), Elsevier, Amsterdam, (2004).
- [4] “Synthesis and characterization of a remarkable ceramic:  $Ti_3SiC_2$ ”, M.W. Barsoum, T. El-Raghy, *J. Am. Ceram. Soc.*, Volume 79, P 1953–1956 (1996).
- [5] “Synthesis and mechanical properties of fully dense  $Ti_2SC$ ”, S. Amini, M.W. Barsoum, T. El-Raghy, *J. Am. Ceram. Soc.*, Volume 90 (12), P 3953–3958 (2007).
- [6] “The  $M_{N+1}AX_N$  phases: a new class of solids; thermodynamically stable nanolaminates”, M. Barsoum, *Prog. Solid State Chem.*, Volume 28, P 201–281 (2000).
- [7] “State of the art on tribological behavior of polymer matrix composites reinforced with natural fibers in the green materials world”, Emad Omrani, Pradeep L. Menezes, Pradeep K. Rohatgi, *Engineering Science and Technology, an International Journal*, Volume 19, P 717–736 (2016).
- [8] “A review on the tensile properties of natural fiber reinforced polymer composites”, H. Ku, H. Wang, N. Pattarachaiyakoop, M. Trada, *Composites: Part B* 42, P 856–873 (2011).
- [9] “Development of HEMP Fiber Reinforced Polypropylene Composites”, Hajnalka Hargitai, *Journal of Thermoplastic Composite Materials*, vol. 21, P 2165-174 (2008).
- [10] “Mechanisms of Friction and Wear Reduction by Carbon Fiber Reinforcement of PEEK”, Xian-Qiang Pei, Roland Bennewitz, Alois K. Schlarb, *Tribology Letters*, 58:42, (2015).

[11] “Natural Fiber Polymer Composites: A Review”, D. N. Saheb, J. P. Jog, *Advances in Polymer Technology*, (1999).

[12] “Mechanical properties of carbon nanotubes based polymer composites”, M. Tarfaoui, K. Lafdi, A. El Moumen, *Composites Part B* 103, P 113-121 (2016).

[13] “Synthesis and Characterization of Novel Al-Matrix Composites Reinforced with  $Ti_3SiC_2$  Particulates” S. Gupta, T. Hammann, R. Johnson, M.F. Riyad, *JMEPEG* 24, P 1011–1017 (2015).

[14] “On the Development of Novel MRM (MAX Reinforced Metal) Multifunctional Materials”, S. Gupta, R. Dunnigan, 11th International Conference on Ceramic Materials and Components (ICACC) for Energy and Environmental Applications, Vancouver, June, P 14-19, (2015).

[15] “Synthesis and Characterization of  $Ti_3SiC_2$  Particulate-Reinforced Novel Zn Matrix Composites”, S. Gupta, M. A. Habib, R. Dunnigan, S. Ghosh, *Journal of Materials Engineering and Performance*, 24, P 4071-4076 (2015).

[16] “Effect of  $Ti_3SiC_2$  Particulates on the Mechanical and Tribological Behavior of Sn Matrix Composites”, T. Hammann, R. Johnson, M. F. Riyad, S. Gupta, The American Ceramic Society, 39<sup>th</sup> International Conference on Advanced Ceramics and Composites, (2015).

[17] “Investigation of the wear behavior of a glass-fiber-reinforced composite and plain polyester resin”, Hasim Pihtili, Nihat Tosun, *Composites Science and Technology*, Volume 62, P 367 -370 (2002).

[18] “Tribological Behavior of Novel  $Ti_3SiC_2$  (Natural Nanolaminates)-Reinforced Epoxy Composites during Dry Sliding”, S. Gupta, T. Hammann, R. Johnson, M. F. Riyad, *Tribology Transactions*, 58: P 560–566, (2015).

## CHAPTER II

[1] “Synthesis and properties of polyaryletherketones”, T.E. Attwood, P.C. Dawson, J.L. Freeman, L.R.J Hoy, J.B. Rose, P.A. Staniland, *Polymer* 22, P 1096–103 (1981).

[2] “Vicatex® poly(ethersulfone) (PES) and Vicatex® poly(etheretherketone) (PEEK)”, O.B. Searle, R. H. Pfeiffer, *Polym Eng Sci* 25, P 474–476 (1985).

[3] “Mechanical properties of poly (ether-ether-ketone) for engineering applications”, D.P. Jones, D.C. Leach, D. R. Moore, *Polymer* 26, P 1385–93 (1985).

[4] “High-performance nanocomposites based on polyetherketones”, A.M. Díez-Pascual, M. Naffakh, C. Marco, G. Ellis, M.A. Gómez-Fatou, *Prog. Mater. Sci.*, 57, P 1106–1190 (2012).

- [5] “Wear and friction behavior of poly-ether-ether-ketone (PEEK) filled with graphene, WS<sub>2</sub> and CNT nanoparticles”, *Wear* 332–333, P 855–862 (2015).
- [6] “Rheology and properties of melt-processed poly (ether ether ketone)/multi-wall carbon nanotube composites”, D. Bangarusampath, H. Ruckdaschel, V. Altstadt, J.K.W. Sandler, D. Garray, M.S.P. Shaffer, *Polymer*, 50, P 5803–5811 (2009).
- [7] “A study on friction and wear characteristics of nanometer Al<sub>2</sub>O<sub>3</sub>/PEEK composites under the dry sliding condition”, H.B. Qiao, Q. Guo, A.G. Tian, G.L. Pan, L.B. Xu, *Tribol. Int.* 40, P 105–110 (2007).
- [8] “PEEK composites reinforced by nano-sized SiO<sub>2</sub> and Al<sub>2</sub>O<sub>3</sub> particulates”, M. Kuo, C. Tsai, J. Huang, M. Chen, *Mater. Chem. Phys.*, 90, P 185–195 (2005).
- [9] “An investigation of the friction and wear properties of nanometer Si<sub>3</sub>N<sub>4</sub> filled PEEK”, Q. H. Wang, J. F. Xu, W.C. Shen, W.M. Liu, *Wear* 196, P 82–86 (1996).
- [10] “The effect of nanometer SiC filler on the tribological behavior of PEEK”, Q.H. Wang, J. F. Xu, W.C. Shen, W.M. Liu, *Wear* 209, P 316–21 (1997).
- [11] “On dry sliding friction and wear behaviour of PEEK and PEEK/SiC-composite coatings”, G. Zhang, H. Liao, H. Li, C. Mateus, J.M. Bordes, C. Coddet, *Wear* 260, P 594–600 (2006).
- [12] “Effect of the reinforcement (carbon or glass fibres) on friction and wear behaviour of the PEEK against steel surface at long dry sliding”, J.P. Davim, R. Cardoso, *Wear* 266, P 795–799, (2009).
- [13] “A low friction and ultra-low wear rate PEEK/PTFE composite”, D.L. Burris, W.G. Sawyer, *Wear* 261, P 410–418 (2006).
- [14] “Morphological and physical properties and friction/wear behavior of h-BN filled PEEK composite coatings”, J. Tharajak, T. Palathai, N. Sombatsompop, *Surf. Coat. Technol.* 273, P 20–29 (2015).
- [15] “The growth and bonding of transfer film and the role of CuS and PTFE in the tribological behavior of PEEK”, J. Vande Voort, S. Bahadur, *Wear* 181, P 212–221 (1995).
- [16] “The wear performance of PEEK-OPTIMA based self-mating couples”, S.C. Scholes, A. Unsworth, *Wear* 268, P 380-387 (2010).
- [17] “Elastic and Mechanical Properties of the MAX Phases”, M.W. Barsoum and M. Radovic *Annu. Rev. Mater. Res.* 41, P 195-227 (2011).

[18] “Synthesis and characterization of a remarkable ceramic:  $Ti_3SiC_2$ ”, M.W. Barsoum, T. El-Raghy, *J. Am. Ceram. Soc.* 79, P 1953–1956 (1996).

[19] “The  $M_{n+1}AX_n$  phases: a new class of solids; thermodynamically stable nanolaminates”, M.W. Barsoum, *Prog. Solid State Chem.* 28, P 201–281 (2000).

[20] “Synthesis and mechanical properties of fully dense  $Ti_2SC$ ”, S. Amini, M.W. Barsoum, T. El-Raghy, *J. Am. Ceram. Soc.* 90 (12), P 3953–3958 (2007).

[21] “On the tribology of the MAX phases and their composites during dry sliding: A review”, S. Gupta and M.W. Barsoum, *Wear* 271, 1878– 1894 (2011).

[22] “ $Ta_2AlC$  and  $Cr_2AlC$  Ag-based composites - New solid lubricant materials for use over a wide temperature range against Ni-based superalloys and alumina”, S. Gupta, D. Filimonov, T. Palanisamy, T. El-Raghy and M. W. Barsoum, *Wear* 262, P 1479-1489 (2007).

[23] “Tribological Behavior of Novel  $Ti_3SiC_2$  (Natural Nanolaminates)-Reinforced Epoxy Composites during Dry Sliding”, S. Gupta, T. Hammann, R. Johnson & M. F. Riyad, *Tribol. T.* 58, P 560-566 (2015).

[24] “Synthesis and Tribological Behavior of Novel UHMWPE- $Ti_3SiC_2$  Composites”, S. Gupta and M. F. Riyad, *Polymer Composites*, (2016).

[25] “Synthesis and Characterization of Novel Al-Matrix Composites Reinforced with  $Ti_3SiC_2$  Particulates”, *J. Mater. Eng. Perform.* 24, P 1011-1017 (2015).

[26] “Synthesis and Characterization of  $Ti_3SiC_2$  Particulate-Reinforced Novel Zn Matrix Composites”, *J. Mater. Eng. Perform.* 24, P 4071-4076 (2015).

### CHAPTER III

[1] “A low friction and ultra-low wear rate PEEK/PTFE composite”, D. L. Burris, W. Gregory Sawyer, *Wear* 261, P 410–418 (2006).

[2] “The friction and wear characteristics of nanometer ZnO filled polytetrafluoroethylene”, F. Li, K. Hu, J. Li, B. Zhao *Wear* 249, P 877–8823 (2002).

[3] “The friction and wear properties of polytetrafluoroethylene filled with ultrafine diamond”, S. Lai, L. Yue, T. Li, Z. Hu, *Wear* 260, P 462–468 (2006).

[4] “Peculiarities of tribological behavior of low-filled composites based on polytetrafluoroethylene (PTFE) and molybdenum disulfide”, V.N. Aderikha, A.P.Krasnov, V.A.Shapovalov, A.S.Golub, *Wear* 320, P 135–142 (2014).

- [5] “Tribological behavior of carbon-nanotube-filled PTFE composites”, W.X. Chen, F. Li, G. Han, J.B. Xia, L.Y. Wang, J.P. Tu, Z.D. Xu, *Tribol. Lett.* 15, P 275–278 (2003).
- [6] “Boric Acid Self-Lubrication of B<sub>2</sub>O<sub>3</sub>-Filled Polymer Composites”, B. R. Burroughs, J. Kim and T. A. Blanchet, *Tribology Transactions* 42, P 592-600 (1999).
- [7] “A study on the friction and wear behavior of PTFE filled with alumina nanoparticles”, W. G. Sawyer, K. D. Freudenberg, P. Bhimaraj. L. S. Schadler, *Wear* 254, P 573–580 (2003).
- [8] “Effect of Particle Size on the Wear Resistance of Alumina-Filled PTFE Micro- and Nanocomposites”, S. E. McElwain, T. A. Blanchet, L. S. Schadler and W. G. Sawyer *Tribology Transactions* 51, P 247-253 (2008).
- [9] “Improved wear resistance in alumina-PTFE nanocomposites with irregular shaped nanoparticles”, D. L. Burris, W. G. Sawyer, *Wear* 260, P 915–918 (2006).
- [10] “Transfer film evolution and its role in promoting ultra-low wear of a PTFE nanocomposite”, J. Ye, H.S.Khare, D.L.Burris, *Wear* 297, P 1095–1102 (2013).
- [11] “Comparison of tribological behavior of nylon composites filled with zinc oxide particles and whiskers”, S. Wang, S. Ge, D. Zhang, *Wear* 266, P 248–254 (2009).
- [12] “Tribological properties of solid lubricants filled glass fiber reinforced polyamide 6 composites”, D. Li, Y. You, X. Deng, W. Li, Y. Xie, *Materials and Design* 46, P 809–815 (2013).
- [13] “Novel melt-processable nylon-6/inorganic fullerene-like WS<sub>2</sub> nanocomposites for critical applications”, M. Naffakha, C. Marco, M. A. Gómez, Ignacio Jiménez, *Materials Chemistry and Physics* 129, P 641– 648 (2011).
- [14] “Effect of carbon fiber reinforcement on the mechanical and tribological properties of polyamide6/polyphenylene sulfide composites”, S. Zhou, Q. Zhang, C. Wua, J. Huang, *Materials and Design* 44, P 493–499 (2013).
- [15] “Elastic and Mechanical Properties of the MAX Phases”, M.W. Barsoum and M. Radovic *Annu. Rev. Mater. Res.* 41, P 195-227 (2011).
- [16] “Synthesis and characterization of a remarkable ceramic: Ti<sub>3</sub>SiC<sub>2</sub>”, M.W. Barsoum, T. El-Raghy, *J. Am. Ceram. Soc.* 79, P 1953–1956 (1996).
- [17] “The M<sub>n+1</sub>AX<sub>n</sub> phases: a new class of solids; thermodynamically stable nanolaminates”, M.W. Barsoum, *Prog. Solid State Chem.* 28, P 201–281 (2000).
- [18] “Synthesis and mechanical properties of fully dense Ti<sub>2</sub>SC”, S. Amini, M.W. Barsoum, T. El-Raghy, *J. Am. Ceram. Soc.* 90 (12), 3953–3958 (2007).

- [19] “On the tribology of the MAX phases and their composites during dry sliding: A review”, S. Gupta and M.W. Barsoum, *Wear* 271, P 1878– 1894 (2011).
- [20] “Ta<sub>2</sub>AlC and Cr<sub>2</sub>AlC Ag-based composites - New solid lubricant materials for use over a wide temperature range against Ni-based superalloys and alumina”, S. Gupta, D. Filimonov, T. Palanisamy, T. El-Raghy and M. W. Barsoum, *Wear* 262, P 1479-1489 (2007).
- [21] “Tribological Behavior of Novel Ti<sub>3</sub>SiC<sub>2</sub> (Natural Nanolaminates)-Reinforced Epoxy Composites during Dry Sliding”, S. Gupta, T. Hammann, R. Johnson & M. F. Riyad, *Tribol. Trans.* 58, P 560-566 (2015).
- [22] “Synthesis and Tribological Behavior of Novel UHMWPE-Ti<sub>3</sub>SiC<sub>2</sub> Composites”, S. Gupta and M. F. Riyad, doi:10.1002/pc.23925 (2016).
- [23] “Synthesis and tribological behavior of novel wear-resistant PEEK–Ti<sub>3</sub>SiC<sub>2</sub> composites”, S. Ghosh, R. Dunnigan and S. Gupta, *Journal of Engineering Tribology*, doi: 10.1177/1350650116648868 (2016).
- [24] “Tribological behaviors of several polymer–polymer sliding combinations under dry friction and oil-lubricated conditions”, B. Jia, T. Li, X. Liu, P. Cong, *Wear* 262, P 1353–1359 (2007).
- [25] “Static friction and adhesion in polymer–polymer microbearings”, Z. Rymuza, Z. Kusznierevicz, T. Solariski, M. Kwacz, S.A. Chizhik, A.V. Goldade, *Wear* 238, P 56–69 (2000).
- [26] “The wear performance of PEEK-OPTIMA based self-mating couples”, S.C. Scholes, A. Unsworth, *Wear* 268, P 380-387 (2010).
- [27] “A tribological assessment of a PEEK based self-mating total cervical disc replacement”, H. Xin, D.E.T.Shepherd, K.D.Dearn, *Wear* 303, P 473–479 (2013).
- [28] “An investigation into PEEK-on-PEEK as a bearing surface candidate for cervical total disc replacement “, *The Spine Journal* 12, P 603–611 (2012).
- [29] “Friction and lubrication of nylon”, R.C. Bowers,W.C. Clinton,W.A. Zisman, *Ind. Eng. Chem.* 46, P 2416–2419 (1954).
- [30] “Adhesion and friction mechanisms of polymer-on-polymer surfaces”, N. Maeda, N.H. Chen, M. Tirrell, J.N. Israelachvili, *Science* 297, P 379–382 (2002).
- [31] “Adhesion and friction of polymer surfaces: the effect of chain ends”, N.H. Chen, N. Maeda, M. Tirrell, J.N. Israelachvili, *Macromolecules* 38, P 3491–3503 (2005).
- [32] “Tribological properties of kaolin filled UHMWPE composites in unlubricated sliding”, Guofang, G. Huayong, Y., Xin, F., *Wear* 256, P 88–94 (2004).

[33] “Changes in tribological performance of high molecular weight high density polyethylene induced by the addition of molybdenum disulphide particles”, Pettarin, V., Churruca, M. J., Felhos, D., Karger-Kocsis, J., Frontini, P. M., *Wear* 269, P 31–45 (2010).

[34] “The development of transfer layers and their role in polymer tribology”, S. Bahadur, *Wear* 245, P 92–99 (2000).

#### **CHAPTER IV**

[1] “Sliding wear behavior and mechanism of ultra-high molecular weight polyethylene”, Wang, Y.Q., Li, J., *Materials Science and Engineering A266*, P 155–160 (1999).

[2] “Tribological properties of kaolin filled UHMWPE composites in unlubricated sliding”, Guofang, G., Huayong, Y., Xin, F., *Wear* 256, P 88–94 (2004).

[3] “Changes in tribological performance of high molecular weight high density polyethylene induced by the addition of molybdenum disulphide particles”, Pettarin, V., Churruca, M. J., Felhos, D., Karger-Kocsis, J., Frontini, P. M., *Wear* 269, P 31–45 (2010).

[4] “State-of-the-art of polymer tribology”, Zhang, S. W., *Tribology International* 31, P 49–60 (1998).

[5] “Synthesis and properties of polyaryletherketones”, T.E. Attwood, P.C. Dawson, J.L. Freeman, L.R.J Hoy, J.B. Rose, P.A. Staniland, *Polymer* 22, P 1096–103 (1981).

[6] “Vitrex® poly(ethersulfone) (PES) and Vitrex® poly(etheretherketone) (PEEK)”, O.B. Searle, R. H. Pfeiffer, *Polym Eng Sci* 25, P 474–486 (1985).

[7] “Mechanical properties of poly (ether-ether-ketone) for engineering applications”, D.P. Jones, D.C. Leach, D. R. Moore, *Polymer* 26, P 1385–1393 (1985).

[8] “High-performance nanocomposites based on polyetherketones”, A.M. Díez-Pascual, M. Naffakh, C. Marco, G. Ellis, M.A. Gómez-Fatou, *Prog. Mater. Sci.*, 57, P 1106–1190 (2012).

[9] “Wear and friction behaviour of poly-ether-ether-ketone (PEEK) filled with graphene, WS<sub>2</sub> and CNT nanoparticles”, M. Kalin, M. Zalaznik, S. Novak, *Wear* 332–333, P 855–862 (2015).

[10] “Rheology and properties of melt-processed poly (ether ether ketone)/multi-wall carbon nanotube composites”, D. Bangarusampath, H. Ruckdaschel, V. Altstadt, J.K.W. Sandler, D. Garray, M.S.P. Shaffer, *Polymer*, 50, P 5803–5811 (2009).

- [11] “A study on friction and wear characteristics of nanometer  $\text{Al}_2\text{O}_3$ /PEEK composites under the dry sliding condition”, H.B. Qiao, Q. Guo, A.G. Tian, G.L. Pan, L.B. Xu, *Tribol. Int.* 40, P 105–110 (2007).
- [12] “PEEK composites reinforced by nano-sized  $\text{SiO}_2$  and  $\text{Al}_2\text{O}_3$  particulates”, M. Kuo, C. Tsai, J. Huang, M. Chen, *Mater. Chem. Phys.*, 90, P 185–195 (2005).
- [13] “An investigation of the friction and wear properties of nanometer  $\text{Si}_3\text{N}_4$  filled PEEK”, Q. H. Wang, J. F. Xu, W.C. Shen, W.M. Liu, *Wear* 196, P 82–96 (1996).
- [14] “The effect of nanometer SiC filler on the tribological behavior of PEEK”, Q.H. Wang, J. F. Xu, W.C. Shen, W.M. Liu, *Wear* 209, P 316–321 (1997).
- [15] “On dry sliding friction and wear behaviour of PEEK and PEEK/SiC-composite coatings”, G. Zhang, H. Liao, H. Li, C. Mateus, J.M. Bordes, C. Coddet, *Wear* 260, P 594–600 (2006).
- [16] “Effect of the reinforcement (carbon or glass fibres) on friction and wear behaviour of the PEEK against steel surface at long dry sliding”, J.P. Davim, R. Cardoso, *Wear* 266, P 795–799, (2009).
- [17] “A low friction and ultra-low wear rate PEEK/PTFE composite”, D.L. Burris, W.G. Sawyer, *Wear* 261, P 410–418 (2006).
- [18] “Morphological and physical properties and friction/wear behavior of h-BN filled PEEK composite coatings”, J. Tharajak, T. Palathai, N. Sombatsompop, *Surf. Coat. Technol.* 273, P 20–29 (2015).
- [19] “The growth and bonding of transfer film and the role of CuS and PTFE in the tribological behavior of PEEK”, J. Vande Voort, S. Bahadur, *Wear* 181, P 212–221 (1995).
- [20] “The friction and wear characteristics of nanometer ZnO filled polytetrafluoroethylene”, F. Li, K. Hu, J. Li, B. Zhao *Wear* 249, P 877–8823 (2002).
- [21] “The friction and wear properties of polytetrafluoroethylene filled with ultrafine diamond”, S. Lai, L. Yue, T. Li, Z. Hu, *Wear* 260, P 462–468 (2006).
- [22] “Peculiarities of tribological behavior of low-filled composites based on polytetrafluoroethylene (PTFE) and molybdenum disulfide”, V.N. Aderikha, A.P.Krasnov, V.A.Shapovalov, A.S.Golub, *Wear* 320, P 135–142 (2014).
- [23] “Static friction and adhesion in polymer–polymer microbearings”, Z. Rymuza, Z. Kusznierevicz, T. Solariski, M. Kwacz, S.A. Chizhik, A.V. Goldade, *Wear* 238, P 56–69 (2000).
- [24] “The wear performance of PEEK-OPTIMA based self-mating couples”, S.C. Scholes, A. Unsworth, *Wear* 268, P 380-387 (2010).

[25] “Synthesis and Tribological Behavior of Novel UHMWPE-Ti<sub>3</sub>SiC<sub>2</sub> Composites”, S. Gupta and M. F. Riyad, Polymer Composites, (2016).

### **PRESENTATION DURING MASTER’S STUDY**

1. “On the Development of Novel Multifunctional MAXPOL Composites”, S. Ghosh, S. Gupta, MS&T 2016, Salt Lake City, Utah.
2. “On the Development of MRMs (MAX Reinforced Metals) for Multifunctional Applications”, F. AlAnazi, S. Ghosh, S. Gupta, MS&T 2016, Salt Lake City, Utah.
3. “On the Design of MAX-Polymer (MAXPOL) Multifunctional Composites”, S. Ghosh, F. AlAnazi, M. Fuka, S. Gupta, ASME Meeting, UND, 2016.
4. “Novel MAX Phase Reinforced Soft Metal Composites”, S Ghosh, R. Dunnigan, Md. Ahsan Habib, S. Gupta, MS&T 2015, Columbus, Ohio.
5. “Novel Metal Matrix Multifunctional Materials by Ti<sub>3</sub>SiC<sub>2</sub> Reinforcements”, Md. Ahsan Habib, R. Dunnigan, S. Ghosh, S. Gupta, MS&T 2015, Columbus, Ohio.
6. “On the Development of MAX Reinforced Metal Matrix Composites”, M. Habib, R. Dunnigan, S. Ghosh, S. Gupta, ICACC 2016, Daytona Beach, Florida.
7. “Development of Novel Additive Manufacturing (AM) Practices”, R. Dunnigan, S. Ghosh, M. Habib, S. Gupta, ICACC 2016, Daytona Beach, Florida.

### **STATUS OF JOURNAL PUBLICATIONS**

1. “Synthesis and Tribological Behavior of Novel Wear Resistant PEEK-Ti<sub>3</sub>SiC<sub>2</sub> composites”, S. Ghosh, R. Dunnigan and S. Gupta, Journal of Engineering Tribology, DOI: 10.1177/1350650116648868.
2. “MAXPOL: Novel solid lubricant materials for multifunctional applications”, Surojit Gupta, M. F. Riyad, Sujan Ghosh, and Ross Dunnigan, Society of Plastics Engineers, 10.2417/spepro.006444.
3. “Synthesis and Characterization of Ti<sub>3</sub>SiC<sub>2</sub> Particulate-Reinforced Novel Zn Matrix Composites”, S. Gupta, R. Dunnigan and S. Ghosh, Journals of Materials Engineering and Performance, DOI: 10.1007/s11665-1691-y.
4. “Novel Self Lubricating Teflon-Ti<sub>3</sub>SiC<sub>2</sub> and Nylon-Ti<sub>3</sub>SiC<sub>2</sub> composites”, S. Ghosh, F. AlAnazi, R. Dunnigan and S. Gupta, Wear (Submitted).

5. "Synthesis and Tribological Behavior of Novel Ag and Bi based MRMs (MAX Reinforced Metals)", F. AlAnazi, S. Ghosh, R. Dunnigan, S. Gupta, Submitted.